Experimental, Numerical Analysis and Parametric Optimization of Press-Brake Bending Process of Perforated Aluminium Alloy (AA)

JIMMA UNIVERSITY

JIMMA INSTITUTE OF TECHNOLOGY

SCHOOL OF POSTGRADUATE STUDIES

A Thesis Submitted to the graduate studies of Jimma University in Partial Fulfilment of the Requirement for the Degree of Master of Science in Mechanical Engineering (Manufacturing System Engineering)

By

Ahmed Jemal Aba Arfesa

ID No 0292/10

October 2020

Jimma, Ethiopia

Experimental, Numerical Analysis and Parametric Optimization of Press-Brake Bending Process of Perforated Aluminium Alloy (AA1300)

Jimma University
Jimma Institute of Technology
School of Postgraduate Studies

A Thesis Submitted to the graduate studies of Jimma University in Partial Fulfilment of the Requirement for the Degree of Master of Science in Mechanical Engineering (Manufacturing System Engineering)

By
Ahmed Jemal Aba Arfesa
ID No: 0292/10

Advisor: Besufekad Negash (Ph. D)
Co advisor: Ahmed Mohammed (MSc.)

October 2020
Jimma, Ethiopia

Declaration

I hereby declare that this thesis: **"Experimental, Numerical Analysis and Parametric Optimization of Press-Brake Bending Process of Perforated Sheet Metal"** is my own work and this work has not been submitted elsewhere for the award of any other degree or diploma. It is being submitted for the degree of Master of Science in Mechanical Engineering (specialization in Manufacturing System engineering), and all sources of material used for this thesis have been dully acknowledged.

Ahmed Jemal		
Name of candidate	*Signature*	*Date*

This thesis has been submitted for examination with my approval as a University Supervisor.

Besufekad Negash (Ph. D)		
Name of Major Advisor	*Signature*	*Date*

Ahmed Mohammed (MSc.)		
Name of Co-Advisor	*Signature*	*Date*
Name of Chairperson	*Signature*	*Date*
Name of Internal Examiner	*Signature*	*Date*
Name of External Examiner	*Signature*	*Date*

Acknowledgment

In the name of Allah, the Most Gracious and the Most Merciful Alhamdulillah, all praises to Allah for the strengths and His blessing in completing this thesis. Special appreciation goes to my supervisor, Dr. Besufekad Negash, for his supervision and constant support. His invaluable help of constructive comments and suggestions throughout the experimental and thesis works have contributed to the success of my research. Not forgotten, my appreciation to my co-supervisor, Mr. Ahmed Mohammed for his support and knowledge regarding this thesis. I would like to express my appreciation to the Dean, School of Mechanical Engineering, Mr. Debala Geneti and to the chair, Manufacturing Engineering, Kancharla Srinivasarao for their support and help towards my postgraduate affairs. My acknowledgment also goes to all the technicians and office staff of the School of Mechanical Engineering for their co-operation.

My deepest gratitude goes to my beloved parents: Mr. Jemal Abarfesa and Ms. Saliya Mohammed. I express my deep gratitude to my wife “Zemzem Mohammed” for immense support during the course of my MSc. Program. Her patience, goodwill, caring nature and encouraging words kept me driving and helped me to focus on my work.

Sincere thanks to all my friends especially Jihad Haji, Mensur Haji, Tamkin Mustafa, and others for their kindness and moral support during my study. Thanks for the friendship and memories. Finally yet importantly, to those who directly or indirectly contributed to this research, your kindness means a lot to me. Thank you very much.

Abstract

Spring-back is one of the problems in the press-brake v-bending process due to the elastic recovery of the material. It can be influenced by various technological, geometrical, and material parameters. In this thesis, the spring-back effect of the press-brake v-bending process of plain and perforated sheet aluminium alloy (AA3003) were conducted and analyzed using FEM and experimental results. It attempts to study the effects of press-brake v-bending process parameters (bend angle and blanks parameters (viz. thickness and pitch perforation) on the formability and spring-back of aluminum alloy. Finite element analysis is done using Abaqus software. Plain and perforated sheet metal is modeled using Solidworks and then imported to Abaqus/CAE where simulation of the press-brake v-bending process were carried. Subsequently, the effects of press-brake bending angle, thickness and pitch perforation were studied based on FEM. The experiments are performed on the hydraulic press brake machine (WC67Y-160X3200). The simulation were compared with experiments that shows permissible limits and it is observed that the experimental results have a good agreement with the simulated ones. Out of all the 36 simulations carried out for plain sheet metal and perforated sheet metal, it is observed that a minimum spring-back value 1.58° is generated for square pitch perforated of 1.5mm thickness. Multi-objective optimization is carried out to determine which group has the best condition for the press- brake v- bending process. Finally, a parametric analysis is carried out using simulation results to optimize process parameters using a multi-objective optimization method. Staggered pitch perforation of 1.5mm thickness having the largest MPI value 1.16×10^{-3} is optimal parameters for 60° bend angle.

Keywords: Aluminium Alloy, V-Bending, FEM, Spring-back, Multi-Objective optimization

Table of Contents

List of Figures

List of Tables

Nomenclature

Roman letters

3D	Three Dimension
C	Center distance between the hole
D	The diameter of the hole
E	Modulus of elasticity
l	Length of workpieces
k	Coefficient of spring-back
t	The thickness of the workpieces
w	Width of workpieces
f_l	Bend depth
L_n	Neutral line
R_P	Punch radius
R_i	Bend radius
e_i	Inner fibers of the material
e_o	Outer fibers of the material

Greek letters

ϕ	Bend angle
ϕ_i	Initial bend angle
ϕ_f	Final bend angle
k	Spring-back factor
α_1	Profile angle

List of abbreviations

AA	Aluminium Alloy
ANOVA	Analysis of variance
ASM	American Standard of Material
CAD	Computer-Aided Design
CAE	Computer-Aided Engineering
C3D8I	Incompatible mode eight-node brick element
DOE	Design of Experiment
EDM	Electron Discharge Machining
EMI	Electro Magnetic Interference
FE	Finite Element
FEA	Finite Element Analysis
FEM	Finite Element Method
HSLA	High Strength and Low Alloy
IGES	Initial Graphics Exchange Specification
MCDM	Multi-Criteria Decision-Making
MPI	Multi-response performance index
PCA	Principal Component Analysis
PMM	Perforated Metal Materials
PP	Pitch Of Perforated
PSM	Perforated Sheet Materials
R3D4	Rigid Three-Dimensional Quadrilateral
RFT	Radio-Frequency Interference
SC8R	8-node hexahedron
T	Thickness
UTM	Universal Testing Machine
WPCA	Weighted Principal Component Analysis
YS	Yield Stress

Chapter One

1. Background

1.1. Introduction

Sheet metal forming is a special case of the deformation process in which sheet metals of less than 6 mm are formed. It is the process of converting a flat sheet of metal into a part of the desired shape without fracture or excessive localized thinning (Abhinav and Annamalai 2013). It has become one of the major manufacturing centers for automobile and aerospace and defense industries, the popularity of sheet metal products is attributable to their lightweight, great interchangeability, good surface finish, and low cost (Iii 2018).

1.2. Bending

Bending is the forming of solid parts, where angled or ring-shaped workpieces are produced from sheet or strip metal. The process consists of uniformly straining flat sheets or strips of metal around a linear axis, but it also may be used to bend tubes, drawn profiles bars, and wire (Boljanovic, 2004). In bending, the plastic state is brought by a bending load. In fact, one of the most common processes for sheet metal forming is bending, which is used not only to form pieces such as L, U or V-profiles but also to improve the stiffness of a piece by increasing its moment of inertia. Bending has the greatest number of applications in the automotive, aircraft and defense industries and for the production of other sheet metal products. Typical examples of sheet-metal bends are illustrated in Figure 1.1.

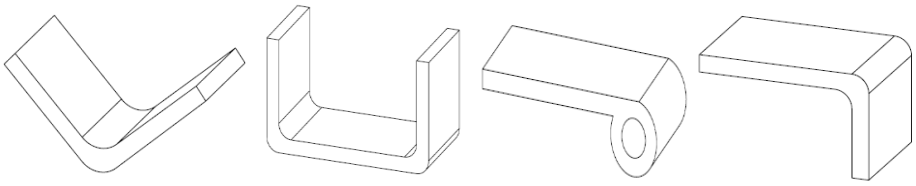

Figure 1.1 Typical examples of sheet-metal bend parts (Boljanovic 2004).

The basic characteristic of bending is stretching (tensile elongation) imposed on the outer surface and compression on the inner surface as shown in Figure 1.2.

In this sense, the terms used in bending are defined in the drawing in Figure 1.3

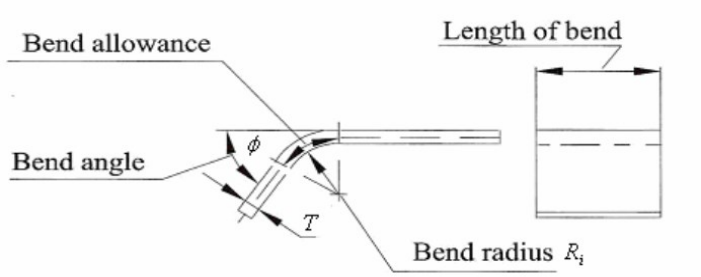

Figure 1.2 Schematic illustrations of terminology, used in the bending process (Boljanovic 2004).

Here, the bend radius R_i measured on the inner surface of the bent piece. The bend angle φ is the angle of the bent piece and T is the material thickness. In bending process, since the outer fibers of the material placed in tension and the inner fibers placed in compression, theoretically, the strain values on the outer and inner fibers are equal in magnitude and given by the following equation:

$$e_o = e_i = \frac{1}{\left(2R_i/T\right)+1} \tag{1.1}$$

Where

R_i = bend radius

T = material thickness.

The deformation in the outer fibers is notably greater, which is why the neutral fibers move to the inner side of the bent piece. The width of the piece on the outer side is smaller and on the inner side is larger than the original width. As R/T decreases, the bend radius becomes smaller; the tensile strain at the outer fibers increases and the material eventually cracks (Boljanovic 2004).

1.3. Spring-back

Ahmed et al. (2014) defined spring-back generally as the undesirable change of part shape that occurs upon removal of constraints after forming. It can consider a dimensional change, which happens during unloading, due to the occurrence of primarily elastic recovery of the part. In other words, (Member et al. 2013) described spring-back as the change in the shape of the formed sheets upon removal from tooling. Spring back is one of the key factors to influence the quality of stamped sheet metal parts in sheet metal manufacturing areas.

1.3.1. Mechanics and Terminology of Spring-back

Every plastic deformation is followed by elastic recovery. Because of this phenomenon, changes occur in the dimensions of the plastic-deformed workpieces upon removing the load. While a workpiece is loaded, it will have the following characteristic dimensions because of plastic deformation shown in Figure 1.8 (Boljanovic 2004).

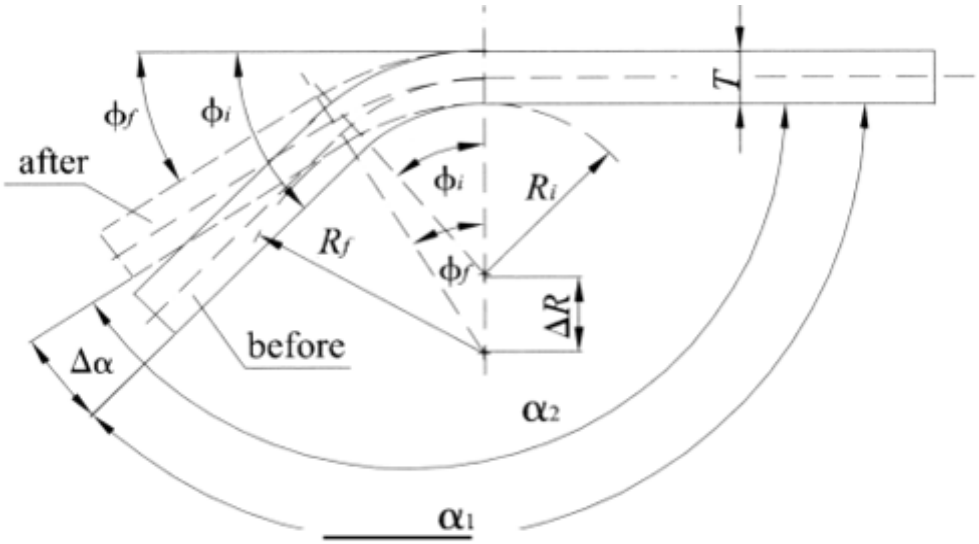

Figure 1.3 Schematic illustration of spring back (Boljanovic, 2004).

Where

- Initial bend radius (R_i)
- Initial bend angle ($\phi_i = 180^0 - \alpha_1$), and
- Initial profile angle (α_1)

All workpieces materials have a finite modulus of elasticity, so each will undergo a certain elastic recovery upon loading. In bending, this recovery is known as a spring-back. The final dimensions of the workpieces after bending unloaded are:

- Final bend Radius (R_f),
- Final bend Angle (α_2), and
- Final profile Angle ($\phi_f = 180^0 - \alpha_2$).

The final angle after spring-back is smaller ($\phi_f < \phi_i$) and the final bend radius is larger ($R_f < R_i$) than before. There are two ways to understand and compensate for spring-back. One is to obtain or develop a predictive model of the amount of spring-back. The other way is to define a quantity to describe the amount of spring-back. A quantity characterizing spring-back is the spring-back factor (K), which is determined as follows:

The bend allowance of the neutral line (L_n) is the same before and after bending, so the following relationship is obtained by the formula:

$$L_n = \left(R_i + \frac{T}{2} \right) \phi_i = \left(R_f + \frac{T}{2} \right) \phi_f \tag{1.2}$$

From this relationship, the spring-back factor is:

$$K = \frac{R_i + \frac{T}{2}}{R_f + \frac{T}{2}} = \frac{\frac{R_i}{T} + 1}{\frac{R_f}{T} + 1} = \frac{\phi_f}{\phi_i} = \frac{180^0 - \alpha_2}{180^0 - \alpha_1} \tag{1.3}$$

The spring back factor (K) depends on R and T. A spring back factor $\mathrm{K} = 1$ indicates no spring back and $\mathrm{K} = 0$ indicates the complete elastic recovery. To estimate spring back, an approximate formula developed in terms of the radii R_i and R_f as follows:

$$\frac{R_i}{R_f} = 4\left(\frac{R_i (YS)}{ET} \right)^3 - 3\left(\frac{R_i (YS)}{ET} \right) + 1 \tag{1.4}$$

Where, *YS is* Yield Stress

E is Modulus of Elasticity

R_P is punch Radius (Boljanovic 2004).

1.4. Perforated Sheet Metals

According to the Handbook Perforated Metals (1993), perforation is a small hole in thin material. There is usually more than one perforation in an organized fashion, where all of the holes collectively are called a perforation. The process of creating perforations is called perforating, which involves puncturing the workpieces with a tool.

1.4.1. Perforation Types and Patterns

Commonly used types of perforations and perforation patterns are discussed below (Mironovs et al. 2017).

a. Perforation Types

- **Round:** Round perforations are produced with the greatest efficiency with less

expensive and more durable tooling. Round holes are the most popular shape in the perforated metal industry. Round perforations are the strongest and most versatile of all perforation patterns.

- **Squares/ Rectangular:** These types of perforations are **v**ery useful in sorting and grading of solid objects, such as grains or minerals. It has the most common use in ventilation and protective guards. Squares are the simplest of all decorative design perforations. The advantages that square and rectangular holes offer are a maximum open area for ventilation, excellent visibility, and excellent protection. Square/rectangular perforations are weaker than round ones (Perforated metal. n.d.).

b. Perforation Patterns

There are 3 types of standard distribution patterns such as 60^0 staggered, 45^0 staggered and rectangular/square (90^0).

- **Staggered:** Distribution of perforations in a triangular pattern, forming at 45^0 or 60^0 angles when joining centerlines of three adjacent holes with a straight line (Figure 1.10a).
- **Rectangular/Square:** Distribution of perforations in a rectangular/square pattern, forming a 90^0 angle when joining centerlines of three adjacent holes with a straight line (Figure 1.10b).

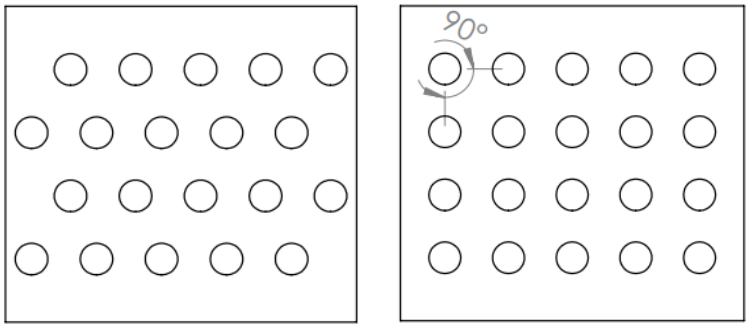

(a) (b)

Figure 1.4 Perforation Patterns (a) staggered perforations in a triangular pattern and (b) Square perforations in a square (Catalog 2015).

c. Open area calculation

An open area is a ratio that reflects how much of the sheet occupied by holes, normally expressed by percent (Perforated Metal. n.d.). It used to calculate for open area per square meter.

Round 45^0 Staggered Center:

$$\frac{157.08 \times D^2}{C^2} = \%0 \tag{1.7}$$

Round 60^0 Staggered Center:

$$\frac{D^2 \times 90.69}{C^2} = \%0 \tag{1.8}$$

Round 90^0 (in straight rows):

$$\frac{D^2 \times 78.54}{C^2} = \%0 \tag{1.9}$$

Where

D = Diameter of the hole

C = Center distance between the hole (Catalogue, n.d.)(Republic, n.d.)

1.4.2. Materials of Perforated Sheet Metals

a. Structural (mild) steel

It is the most cost-effective material and its surface can be done in a variety of finishes – powder painting, galvanizing, hot-dip galvanizing, painting, etc.

b. Stainless steel

It guarantees along working life and it does not corrode. It is mainly used in pharmaceutical, food processing and chemical industries production lines that are required to observe strict sanitary regulations, but they are also used in modern architecture.

c. Galvanized steel

It used for structural steel that is coated with zinc. Its surface can be done in a variety of finishes such as powder paint and other coatings. It is commonly used for ventilation and air-conditioning devices, in manufacturing soundproof rooms and walls.

d. Aluminum

It is used when lightweight materials are required. It has a long working life and it does not corrode. It can be anodized painted with powder paint for an attractive look and a permanent gloss (Specifiers And Buyers Handbook For Perforated Metals 1993).

1.4.3. Advantages of the perforated sheet metal

According to (European Perforators Association. n.d.) The advantages of perforated plates are discussed below.

- **Reduction in Weight:** Reducing weight is becoming more important in areas such as the aerospace industry. The perforated metal is the ideal way to meet this requirement. In addition, machining a perforated plate (bending, etc.) does not leave its load-carrying capacity at a disadvantage compared to the unperforated specimen.
- **Ease in Separating Materials:** The perforation and open area can be specified exactly, making the perforated sheet ideal for filtering, separating, or sorting goods. The open area can be varied in numerous ways to affect the flow rate, size sorting, etc. accurately. Filter elements made from perforated metal are of major benefit to the user.
- **Enhanced Heat Dissipation:** Components made from perforated sheets play a valuable role in regulating temperature by the heat dissipation in cold shelves, hot-air ventilators or complex heating units. The combination of useful functions with an appealing design gives rise to solutions in which a unique aesthetic touch complements the actual function of the application.
- **Enhanced Acoustic Performance:** The Perforated plate is used for soundproofing and for reducing acoustic emissions. Almost all the results required can be achieved by defining the open area accurately. The perforated sheet is even ideal as supporting material for other sound-insulating applications.
- **Radiation Containment:** The Perforated plate is used to enclose electrical appliances in order to attenuate the emitted EMI /RFT radiation and to ventilate the appliances at the same time
- **Improved Skid Resistance / Anti-Skid:** Floor coverings made from the perforated or stamped plates have special anti-skid properties to ensure safety in many areas. Especially in areas with high exposure to wetness, dirt, etc., perforated floor coverings and steps, etc. offer excellent skid-resistance so you can walk across these dangerous surfaces safely.

1.5. Aluminium Alloys

Now days, there is a great concern about a weight reduction of automobiles and construction due to the increased production of aluminium alloys with better formability. Aluminium alloy sheets are being ideally employed in making components for automobiles and shipbuilding due to their excellent properties such as high specific strength, corrosion resistance, and weldability (Davis 2001)

1.5.1. Common Types of Aluminum Alloys

Table 1.1 Applications of Common Types of Aluminum Alloys (Hirsch 2014)

A. Alloys	**Applications**
1100	It is commercially pure aluminum with a content of 99.0%. Its strength is relatively low but has excellent ductility, formability, weldability, and corrosion resistance.
1300	The primary uses of the 1300 series applications are in which the combination of extremely high corrosion resistance and formability are required (e.g., foil and strip for packaging, chemical equipment, tank car or truck bodies, spun hollowware, and elaborate sheet metal work).
2024	Belongs to the Al-Cu-Mg alloy. High-strength hard aluminum, which is twice hard than 5052.
3003	It is an alloy of aluminum and manganese. It is the most widely used anti-rust aluminum. It has good corrosion resistance (close to 1100) to atmospheric, freshwater, seawater, food, organic acid, gasoline, etc.
5005	Similar to 3003. It has medium strength and good corrosion resistance, and its anodized film is brighter than 3003.
5052	Belongs to the Al-Mg alloy and has a wide range of applications. Especially in the construction industry, it is the most promising alloy.
6061	Belongs to the Al-Mg-Si alloy. It has many features: Excellent processing properties, good corrosion resistance.
7075	It is a cold-treated forging alloy with high strength and hardness, far better than mild steel. It is one of the most powerful alloys in the industry, with common corrosion resistance, good mechanical properties, and excellent anodic reaction.

1.6. Optimization

Most industrial processes and products have more than one quality characteristic. To select the best design, it is necessary to consider all characteristics of quality simultaneously, known as multi-objective optimization.

1.6.1. Multi-Objective Optimization

In solving a multi-objective optimization problem, the optimum design parameters' settings

searched for a product or a process in such a manner that the product characteristic or response attains its desired target with minimum variation. A wide range of multi-objective optimization techniques, also sometimes called multi-criteria decision-making (MCDM) techniques.

The dimensionality reduction strategy is one of the numerical techniques for the optimization of multiple responses. It aggregates multiple responses into a single dimensionless measure so that a problem in the optimization of multiple responses then converted into a single objective optimization problem. The single aggregated measure has generally defined as the desirability function. The desirability method recommended due to its simplicity, availability of software. It provides flexibility in weighting and giving importance to individual responses(Liao, 2006).

1.7. Objectives of the Research

1.7.1. General Objectives

The objective of this research is to study experimental, numerical analysis and parametric optimization of the process parameters of press-brake bending process.

1.7.2. Specific Objectives

1. To model bending and simulate of process of press brake bending process.
2. To perform experimental analysis of press brake bending process.
3. To predict spring-back for the press brake v-bending process of perforated AA using FEM.
4. To optimize process parameters for the press-brake v-bending process of perforated AA sheet metal.

1.8. Scope of the Research

- Material for experiment is cut in transverse direction.
- Circular hole of 5mm diameter is used for perforation with different arrangements.
- Ligament width of perforation is 10mm.
- The effect Process parameters such as bending angle, blank thickness, and circular hole with a different pattern of perforation are used.
- Spring-back measured experimentally using bevel protractor and FEM using abaqus.

1.9. Structure of the Research

The work performed in the present thesis consists of six chapters. This chapter has presented an Introduction to the metal forming and scope of the thesis. Chapter 2 presents a literature review on the press brake v-bending process and a detailed summary of the techniques used to simulate the spring-back of the v-bending process. It discusses a number of mechanisms of press brake bending; processes of press brake bending, the effect of process parameters on the v-bending process, and effects of perforation on the v-bending process, and process modeling of press-brake bending processes. Chapter 3 detailed description regarding experiments and simulations of press brake bending. The experimental setup, testing machine and details of numerical simulation have been explained. Chapter 4 results and discussion on the result of the experiment and FEM simulation. Chapter 5 presents the optimization of process parameters of the press brake V-bending process of aluminium alloy. Conclusions and scope for future work are presented in Chapter 6 followed by references and appendices.

Chapter Two

2. Literature Review

2.1. Introduction

Forming is a widely used manufacturing process in many industries for the fabrication of a wide range of products. This process is used more because metal can be formed in any useful shape easily by plastic deformation. Perforated sheet metal is having less weight and the same strength compare to the plain sheet. It is widely used in screens, filters, shields, and guards. It is also used in architectural design (Kaneriya et al. 2017).

2.2. Bending Mechanism

Technology et al. (1993) reported Sheet metal forming processes are widely used by the automotive and aerospace industries. More than 55% of sheet metal components are produced by press-brake bending in these industries. Press-brake bending is a sheet metal forming process where the sheet is subjected to a bending load, can perform different operations such as V-bending, U-drawing, channel dies bending and wiping-die bending which also known as L is bending. It is operated by placing the metal sheet (a blank) over a die and the punch then travels down, pressing the blank into the die cavity**.** Miranda et al. (2018) studied press brake air bending, a process of obtaining products by sheet metal forming can be considered at first sight a simple geometric problem. However, the accuracy of the obtained geometries involves the combination of multiple parameters directly associated with the tools and the processing parameters, as well as with the sheet metal materials and dimensions. They concluded that It is possible to predict efficient and accurate final geometries after bending, being also a step forward to a ‘‘first time right’’ solution. In addition, they developed models, methodologies and obtained results were validated by comparison with experimental tests.

2.3. Process Parameters

2.3.1. Material Condition

Trzepiecinski and Lemu (2017) conducted the test on specimens that were cut in the rolling direction (0°) and transverse direction (90°) of the sheet metal and the blank cut along the transverse direction exhibits greater spring-back, than the blank cut in the rolling direction. These results were found both experimentally and by FE models. However, in all analyzed cases,

numerical models over predict the spring-back coefficient value. A decreasing spring-back coefficient is observed when the relative bending depth *(w/f)* increases.

Sheet thickness is a very important variable parameter affecting spring-back and residual stresses. Nandedkar et al. (2015) reported on sheet metal bending; the spring-back phenomenon leads to undesired effects on the geometry and dimensions of the formed parts. One of the main causes that lead and influence the intensity of this instability phenomenon is the state of residual stresses generated by the bending process in the deformed material.

Panthi et al. (2010) described spring-back highly depends on material properties (yield stress, Young's modulus, strain hardening) and geometric parameters (thickness of the sheet, die radius, sector angle) at minimal load condition and it decreases with an increase in compression depth. It shows that near net shape can be achieved by properly controlling the forming load. It is observed that any combination of material and geometry becomes irrelevant after a certain forming load/compression depth. Spring-back increases with an increase in sector angle. Friction has a negligible effect on spring back. The spring back increases with an increase in yield stress, strain hardening, but it decreases with an increase in Young's modulus.

Dametew and Gebresenbet (2016) described spring back is the main defect in the sheet metal bending process. The spring-back of sheet metal bending, which is defined as elastic recovery of the part during unloading conditions. It should be taken into considerations to produce bent sheet metal parts with acceptable quality. Spring-back is affected by factors such as; sheet thickness, tooling geometry, friction condition; material property and processing parameters. Numerical investigation of Spring-back on edge bending die process is done using ANSYS™ LS-DYNA™. Concluded that, increasing of sheet metal strength the spring-back increases. Aluminium exhibits lower spring back than mild steel and high strength sheet metals. For decreasing the tool radius leads to spring back is reduced.

Dilip Kumar et al. (2014) investigated metal forming operation; the flow of material within the body is responsible for bringing about the permanent shape change. The developed finite element model has been used for numerical modeling of the sheet metal L bending operation. From the result, the severity of the thinning problem and spring back effect can be easily identified. Experiments are conducted for different thicknesses and clearance between the die and punch and the results are closely scrutinized with the results obtained by the finite element method.

Prabhakar et al. (2013) reported the spring-back phenomenon in the metal forming process

using Finite Element Analysis. Spring-back phenomenon is an undesirable process in the manufacturing industry. Many parameters influence the spring-back phenomenon. Sheet metal thickness and depth of forming effect on spring back are analyzed using Finite element methods. The results show plate thickness has an effect on all these parameters. With the increase of the plate thickness, spring back, percentage spring back, von-Mises stress, residual stress, contact pressure, and plastic strains are reducing which is an important parameter to obtain better products.

2.3.2. Tool Geometry

Gupta and Reddy (2017) evaluated the effects of technological parameters used in the v-die bending process, on the obtained product properties and dimensions. By variation of the tool geometry, several cases of steel sheet bending process are observed through the FEM simulations. Bend radius or Die radius R_i, is one of the most important parameters, which considerably affects all bending operations of sheet metals. The bend radius in bending operations always pertains to the inside radius of the bend. Ahmed et al. (2014) reported the minimum bend radius is dependent on the material thickness and the mechanical properties of the material. Minimum bend radii vary for various metals; generally, most annealed metals can be bent to a radius equal to the thickness, T and sometimes to 2T, for a given bend angle and bend length. Bend angle is another crucial factor in bending operations. Nandedkar et al. (2015) studied Residual stresses & Spring-back in sheet metal bending depends upon different variable parameters like punch angle, sheet thickness, punch tip radius, punch height, bending force, clearance between punch and die, sheet anisotropy, etc. It is observed that sheet thickness is a very important variable parameter affecting spring-back and residual stresses. The punch tip radius is also affecting spring back and residual stress due to the yielding of material.

Buang et al. (2015) carried out using two sets of experiments and the DOE method, the results show that punch and die radii are significant factors affecting spring-back in stainless steel sheet metal in air v-die free bending. From the analysis and the results of the experiments, it concluded that the punch radius is a more significant factor affecting spring-back. Spring-back increases with the increase in the punch and dies radii. In the air v-die free bending process, the punch radius is the most important factor to be considered. The experimental method agreed well with the DOE results. Panda and Pawar (2018) analyzed and studied four process parameters like punch angle, die opening, grain direction and pre-bend condition of strip affecting on spring-back in the v-bending process for deep draw steel HSLA 420 and St12 are using FEM simulation, Taguchi, and

the ANOVA techniques. The results obtained through FEM simulation are validated by Laboratory experimentation. From the above study, it is observed that two process parameters punch angle and die opening had a major influence on spring back.

The variation of the spring-back coefficient value almost shows linear dependence between the spring-back coefficient values and the bend angle under loading (Trzepiecinski and Lemu 2017). Choudhury and Ghomi (2014) reported spring-back is the difference between the bent angle after the removal of load and the die angle equation (2.1).

$$\text{spring-back} = \phi_f - \phi_i \tag{2.1}$$

Billade and Dahake (2018) observed the forming process of sheet metal component defects such as wrinkles and thinning. These defects can be reduced by varying the process parameters by trial and error method which loss in time and money. The final component is obtained in its desired quality by optimizing the various process parameters, which affect more on the forming process. This requires a thorough knowledge of the process and expertise in tool design. Kaneriya et al. (2017) Observed wrinkling and stress intensity at the curved portion are the major problems, which decrease the life of the product.

2.3.3. Effects of Perforation on Forming

The deformation behavior of perforated sheet metals depends on the geometry of the perforations and on their arrangements (Chen, 1993). According to (Elangovan & Narayanan, 2010) forming limit strains is increased with the ligament width and decreased with the diameter of the perforations.

Narayanan (2012) worked on commercial pure aluminium perforated sheets that were considered, for V-bending analysis. The influences of the presence of holes on the spring-back angle in the sheet metals were investigated. Spring-back angles of these sheets were found out using Finite Element Analysis. The influences of hole size, hole shape, and arrangement of holes of sheets on spring-back angles were studied. It has been found that spring-back decreases when hole size increases. Sheets with square holes exhibit more spring-back than that of circular holes. Spring-back of sheets with holes arranged in the triangular pattern is less than that of holes arranged in a square pattern.

Farsi and Arezoo (2011) investigated the influence of the area of the holes, die angles, die

widths and punch radius on the value of the spring-back and the bending forces in v-die bending. According to the results obtained from the experiments, the spring-back is a function of material thickness, die and punch angle, punch radius, die width and the size of the punched hole. The size of the hole on the bending surface has an effect on the bending angle. When the size of the hole is increased, the final angle of the part is decreased.

Uniyal et al. (2016) studied spring-back analysis of perforated steel sheet metal having circular holes arranged in the square pattern using finite element analysis. An attempt is made to study the effect of various parameters like percentage of open area, hole size and blank thickness on spring-back of formed perforated steel. Concluded that for the spring-back effect on perforated steel sheets. The spring-back effect value increases with an increase in the size of the hole. The spring-back effect value decreases with an increase in the thickness of the blank. The spring-back effect value increases with an increase in the percentage of open area and then decreases.

Venkatachalam et al. (2016) studied the influence of parameters like percentage of open area, hole size and sheet thickness on the forming behavior of perforated sheet metal are studied. It is inferred that the draw depth increases with the percentage of open area. But an increase in hole size and sheet thickness increases the draw depth initially but decreases after some values.

Elangovan et al. (2010) studied the forming limit diagram of perforated commercially pure aluminium sheet under a different mode of deformation. The limit strains of the unperforated sheets are higher than of the perforated sheets in all modes of plastic deformation, and there is a uniform variation in the limit strain ratio. The formability of the perforated sheet depends on ligament ratio and percentage of open area, and as the ligament ratio increases or as a percentage of open area decreases, the formability increases marginally.

Venkatachalam et al. (2016) investigated the influence of parameters like percentage of open area, hole size, and thickness of sheet on the draw depth and thinning of square hole perforated sheet metal. The percentage of error of FEA results when compared to experimental results are within permissible limits. The percentage of thickness reduction slightly increases and then decreases significantly when the percentage of open area increases. It is also inferred that the percentage thickness reduction is directly proportional to the hole size. When the thickness of the sheet is increased, the percentage thickness reduction decreases. In addition, there is a subsequent increase in the percentage of thickness reduction when the thickness of the sheet is further increased.

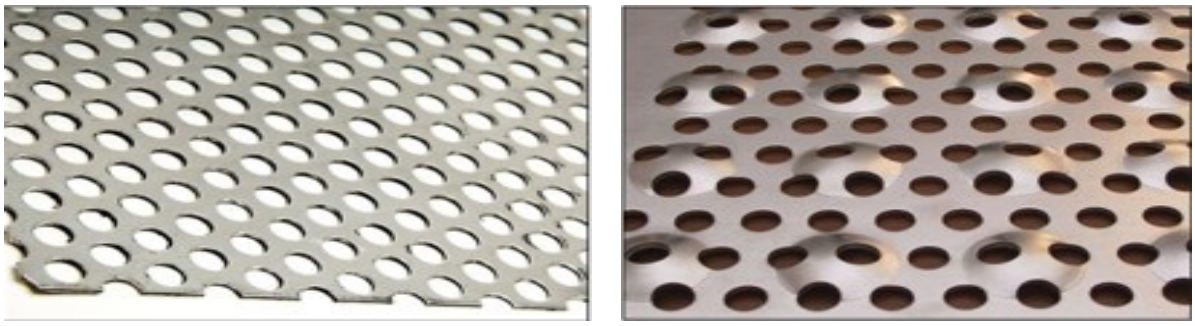

(a) (b)

Figure 2.1 Perforated sheet metal: (a) before the deep draw and (b) after the deep draw (Venkatachalam et al. (2016)

Ling et al. (2016) conducted experiments on forming of punched holes and concluded that: The spring-back is a function of material thickness, die and punch angle, punch radius, die width and the size of the punched hole. The difference between the die and punch angle is important in perforated components bending operations. When that is increased, the spring-back is increased too. Under the same conditions, the spring-back for the parts with less thickness is greater than the parts with more thickness.

2.4. Materials used for Perforation

Systems and Academy (n.d.) reported perforated metallic materials to have a big potential to be used in different building construction. Stiffness, strength and elastic/plastic properties of perforated metallic materials open up good opportunities for their wide range of use in the building industry. Jo et al. (2009) studied perforated metal materials (PMM) that combine a range of properties, including rigidity, strength, lightweight, small thickness, dosed transparency, and decorative attractiveness. All these bring new application effects in the construction industry and architecture. Nowadays, PMM is widely used in the design of facades and interiors all over the world, becoming more popular in Latvia as well. The paper touches several aspects of PMM applications, including its decoration function, shadowing of sunlight, sound and noise barrier function and the problem of corrosion when exploited outdoors.

Sayed (2019) studied perforated steels under the influence of uniaxial tensile load. Because of the presence of these perforated steel sheets, the characteristics of the steel sheets will either increase or decrease. The effect of the perforated staggered shape on the stresses and modulus of elasticity has the opposite effect as it reduces the stress and modulus of elasticity. Kothari and Jhala (2016) Studied finite element analysis of the forming the process of steel perforated sheet

metal (PSM). Simulations were conducted to scrutinize the impact of material thickness, type of blank, blank shape, shape & pattern of perforation, the pitch of perforation, etc. on stress and load-displacement curve for a set of results. The numerical method was used to determine optimum results with reference to process parameters as blank thickness, Punch velocity and stress distribution during the process on the sheet metal.

Uniyal et al. (2016) reported for the spring-back effect on perforated steel sheets. The spring-back effect value increases with an increase in the size of the hole. The spring-back effect value decreases with an increase in the thickness of the blank. The spring-back effect value increases with an increase in the percentage of open area and then decreases.

Venkatachalam et al. (2012) worked on commercial pure aluminium perforated sheets with circular and square holes that were modeled. Limiting strains of these sheets were found out using Finite Element Analysis. The influences of open area, pattern in which holes are arranged and shape of the holes on limiting strains are studied. In the case of open area, the results obtained from FE analysis is confirmed with experimental results. It has been found that limiting strain decreases when open area decreases whereas it increases when the holes are arranged in a triangular pattern rather than the square pattern. Also limiting strain is high for circular holes than for square holes. Narayanan (2012) reported on commercial pure aluminium perforated sheets were considered, for V-bending analysis, in this work. The influences of the presence of holes on the spring-back angle in the sheet metals were investigated. Spring-back angles of these sheets were found out using Finite Element Analysis. The influences of hole size, hole shape, and arrangement of holes of sheets on spring-back angles were studied. It has been found that spring-back decreases when hole size increases. Sheets with square holes exhibit more spring-back than that of circular holes. Spring-back of sheets with holes arranged in the triangular pattern is less than that of holes arranged in a square pattern.

2.5. Processes Model

Gupta and Reddy (2017) studied the FEA of V-bending with the help of LS Dyna. As the thickness increases for the same bend angle spring back is also increases. In addition, it has been observed that as the bend angle increases for the same thickness the Spring-back is increased.

Gite et al. (2016) observed Von-Misses stress in each case reaches a maximum limit and then reduces depending on the thickness and bend angle. The total plastic strain increases to a maximum value and remains stable. From the results obtained by finite element analysis and

experimental validation of the spring-back effect of pivot bracket, it can conclude that the spring-back effect (elastic recovery) of sheet metal varies with the die valley angle and punch nose radius. With the increase of the die angles, spring back, percentage spring back, von-Mises stress, residual stress, contact pressure, and plastic strains are increasing.

Thipprakmas (2010) applied FEM simulation to investigate the spring-back and spring-go phenomena in a v-die bending process and to investigate the effects of process parameters, including the radius and height of the punch. The FEM-simulation results were validated by laboratory experiments. The FEM-simulation results showed that the spring-back and spring-go phenomena could be theoretically elucidated based on material-flow and stress-distribution analyses. The generation of an S-curve-shaped material-flow feature caused the reversal of stress distribution on the leg of the workpieces.

Pal and Rao (2016) reported finite element simulation results are in line with the experimental results. In addition, it is found that when there is a significant amount of spring, the simulation results and experiment results are in close approximation with each other. Hence, it is concluded that the finite element simulation can be used for the prediction of spring back prior to the forming operation using FE tools.

Biradar and Deshpande (2012) investigated of Finite element analysis of sheet metal forming; it shows that the die radius has a significant amount of effect on the spring-back. The results from analysis for die shoulder shown that the increase in die shoulder radius increases the spring-back hence to avoid the spring-back use of a smaller die radius is recommended from this study. In addition, the punch nose radius has a significant effect on the spring-back, up to certain punch nose radius though it does not have much effect as compared to the die radius on spring-back.

Abaqus is one of the adaptable Finite Element Analysis software that can be used to model structures both homogenous and heterogeneous, on a macro as well as a micro-scale. Khamis and Bahari (2016) developed numerical simulations to improve the spring-back prediction by Finite Element analysis, guidelines regarding the mesh discretization provided and a new through-thickness integration scheme for shell elements is launched. Cui et al. (2019) carried out the Abaqus/explicit software that was used to calculate the quasi-static stamping and dynamic deformation process. When the deformation is terminated, the spring-back of the sheet is calculated by Abaqus/implicit software. Florica et al. (2007) used the Finite Element Method

(FEM) to evaluate the spring-back, as well as the stress state in the part before and after the spring-back by using Abaqus Standard.

Trzepiecinski and Lemu (2017) reported the numerical model to indicate that five integration points are the minimum acceptable considering the computation time and accuracy of spring-back prediction. Analyses of the sheet material with seven or more integration points through the thickness indicated that both Simpson's and Gauss's rules provide similar accuracy of prediction. The Gauss' rule with five integration points is optimal to obtain the accurate results of spring-back prediction. The friction coefficient value slightly influences the spring-back amounts.

Coër et al. (n.d.) conducted to perform two types of finite elements: the C3D8I linear hexahedron element with selectively reduced integration to which incompatible deformation modes are added; and the SC8R solid-shell with reduced integration (only 1 integration point in the plane), combined with the Simpson integration rule, considering 5 and 15 through-thickness points. The SC8R element is more cost-effective since all the experimental results are globally predicted, with a much smaller computational time (factor of 4.15 between the SC8R and C3D8I elements). However, the use of only one element through-thickness makes it impossible to predict the thinning zones.

2.6. Process Optimization

Quality plays a significant role in today's mechanized world due to the intricate operational environment and situation linked to the use of sheet metal parts (Reddy et al.2015).

Joshi et al. (n.d.) reported optimization of process parameters in sheet metal forming is an important task to reduce manufacturing cost. To determine the optimum values of the process parameters, it is essential to find their influence on the deformation behavior of the sheet metal.

Bhagyashri R. Billade (2018) analyzed the strain and thickness variations using the Finite element method (FEM) during the forming process and optimization is carried out using the Design of experiment (DOE) technique. The optimization of process parameters is done by using DOE by Taguchi's orthogonal arrays in Minitab software. The result of the optimization is validated with actually formed components with the same optimized parameters. Ling et al. (2016) presented the application of the Taguchi method to analyze the effect of several parameters on the spring-back.

Elangovan and Narayanan (2010) optimized experimental results of perforated sheets using

statistical analysis of ANOVA. Thipprakmas and Phanitwong (2011) investigated the process parameters used in the v-bending process such as bending angle, material thickness, and punch radius using FEM simulation, in association with the Taguchi and the ANOVA techniques. The combination of the FEM simulation, the Taguchi method, and the ANOVA technique was an effective tool to predict the degree of importance of the process parameters in the V-bending process, in addition to aiding in the improvement of the quality of the required bending angle by optimization of the process parameters relating to the spring-back. Venkatachalam et al. (2016) employed the ANOVA technique to study the level of influence of hole size and percentage of open area parameter on the Z-direction displacement and percentage thickness reduction.

(Kothari and Jhala, 2016) used Weighted Principal Component Analysis, a multi-response objective optimization method to derive the best parameters for minimizing the induced stress value. Liao (2006) carried out a WPC method to improve the multi-response problem in the Taguchi method. Most importantly, the proposed WPC method not only reduces the uncertainty and complexity of engineers' judgment associated with the Taguchi method but also overcomes the shortcomings of the PCA method.

2.7. Major Gap from Literature

From the literature review of Perforated Sheet Metal, there is a significant influence of parameters like the die radius, punch radius, blank thickness, bending angle, pitch (pattern) of perforation and effective die width on the output parameters, like induced stress during the forming process, spring-back and bending force bending process. In addition, few of the common methods like Taguchi, ANOVA, and Surface Response Methodology techniques are used for the optimization of process parameters.

Current research is concerned with the experimental, numerical analysis and parametric optimization of the press brake v-bending process-perforated AA. The Process parameters such as bending angle, blank thickness and circular geometry with a different pattern of perforation on spring-back are analyzed. Process parameters of the press brake v-bending process of AA plain and circular holes with the different pitch of perforation are optimized using multi-objective optimization. Due to the reasons of there is no research paper on the circular pitch (pattern) of perforation. No numerical model and simulation for effective prediction of press brake bending process.

Chapter Three

3. Details of Experiments and FEM Procedures

3.1. Introduction

This chapter discusses the experimental setup for press brake v bending process and its modeling by the finite element method (FEM). Details of the experimental setup, working procedure and methods, workpieces geometries and bending parameters are discussed. The FEM simulations are validated by using the experimental work. This chapter discusses the methodology of experiments and FEM simulations. It also discusses how the mesh sensitivity analysis was carried out. The chapter only focuses on methodology, the research findings are reported in the subsequent chapters.

3.2. Chemical Compositions of the Materials

In this research, work materials selected for the study- aluminium alloy. The chemical compositions of aluminum alloy analyzed using a Spectromax$_x$ metal analyzer.

3.2.1. Spectromax$_x$ Metal Analyzer

The principle of the analytical method of Spectro´S Stationary Metal Analyzers is optical emission spectroscopy. The optical emission involves applying electrical energy in the form of spark generated between an electrode and a metal sample, whereby the vaporized atoms are brought to high-energy state within a so-called discharge plasma. The sample material is vaporized on the spark stand by an arc or spark discharge. The atoms and ions contained in the atomic vapor are excited into the emission of radiation. The radiation emitted is passed to the spectrometer optics via an optical fiber, where it is dispersed into its spectral components. From the range of wavelengths emitted by each element, the most suitable line for the application is measured by means of a photomultiplier.

The radiation intensity, which is proportional to the concentration of the element in the sample, is recalculated internally from a stored set of calibration curves and can be shown directly as percent concentration shown in Figure 3.1.

The important specifications of Spectromax$_x$ are given in Appendix A.

Figure 3.1 Spectromax$_x$ Ametek metal analyzer (Ethiopia commodity assessment enterprise)

- **Spark Analyzer Vision Software**

  The Windows Spark Analyzer Vision instrument software from the Spectro lab high-performance spectrometer is used in the Spectromax$_x$. It provides a simple, intuitive interface with numerous functions for the setting of instrument parameters, for data exchange with external computers and for the printing and evaluation of results based on an integrated SQL databank as shown in Figure 3.2.

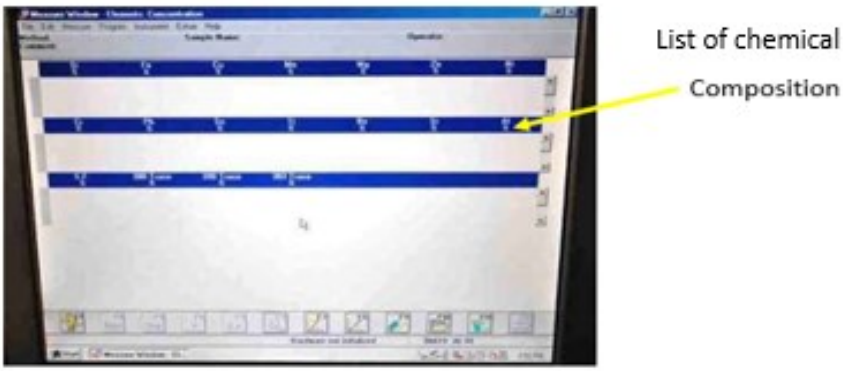

Figure 3.2 Spark analyzer vision software (Ethiopia commodity assessment enterprise)

The chemical composition aluminium alloy in weight percentage was obtained from the Spectromax$_x$ as shown in Table 3.2.1

Table 3.1 Chemical composition of aluminum alloy

Al	Fe	Si	Cu	Li	Ti	Mn
99.2 %	0.43 %	0.16 %	0.058 %	0.016	0.021	0.12

3.3. Study on Mechanical Properties of Workpieces

The mechanical properties like tensile strength and percentage elongation of raw samples are evaluated. Mechanical properties of aluminum alloy measured using the tensile testing machine.

3.3.1. Universal Testing Machine

In order to measure the mechanical properties of aluminum alloy, uniaxial tensile tests were carried out according to the ASTM standard. All the samples were tested in the Universal Testing Machine (UTM) shown Figure 3.3. The important specifications of the universal testing machine are given in Appendix B.

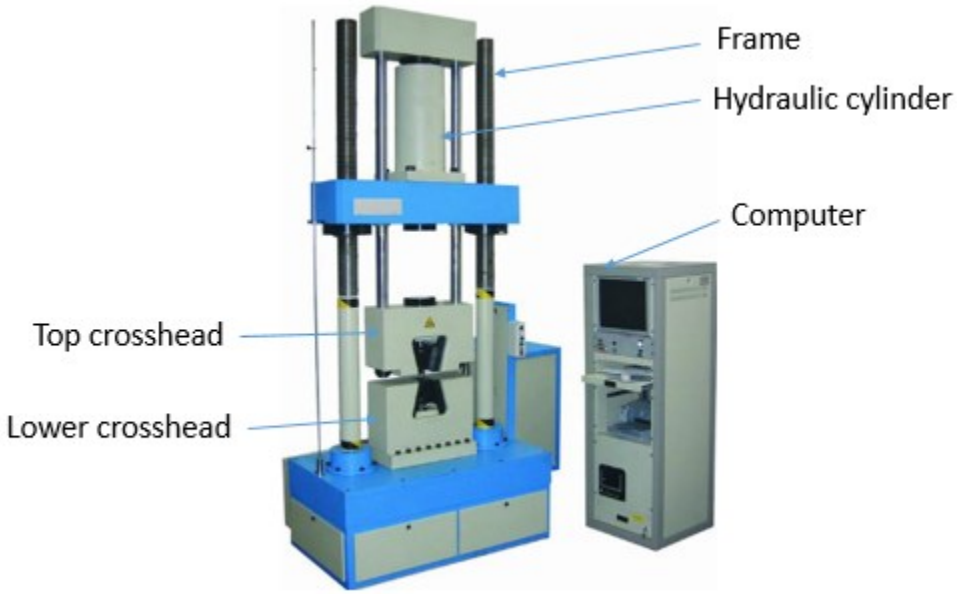

Figure 3.3 Universal Testing Machines of Erie DI-CP (Ethiopia commodity assessment enterprise)

- **Specimen for tensile test**

  The specimen prepared according to the ASM standard of designation E8/E8M - 16a shown in Figure 3.4 (ASTM E8, 2010). All thicknesses are in millimeters (mm).

  The spring-back is greater in transverse direction (Trzepiecinski and Lemu, 2017). Due to this sample, sheets were cut along the transverse direction (90^0) with wire EDM to avoid heating up of samples due to frictional force to the required shape as shown in the Figure 3.5 to determine the mechanical property. It was then cleaned thoroughly with soapy water, rinsed in warm water to remove up dirt, and then conduct by using of the "Universal Testing Machines of Erie DI-CP".

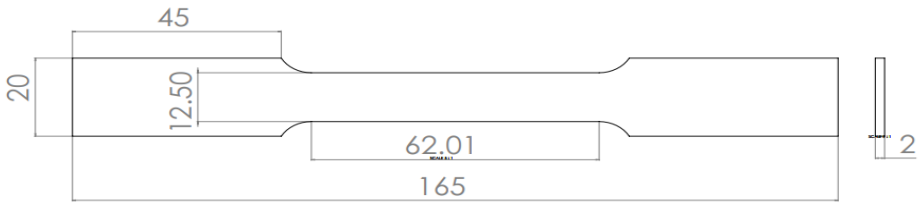

Figure 3.4 The specimen dimension according to ASM standards

Figure 3.5 Specimen for the tensile test

The Figure 3.6 shows samples were positioned in the jaw of the tensile testing machine using the rack and pinion type Flat Grips for testing flat specimens. The grip retainers were assembled at the top and lower crossheads placed in position and loosely fastened the screws holding the retainers.

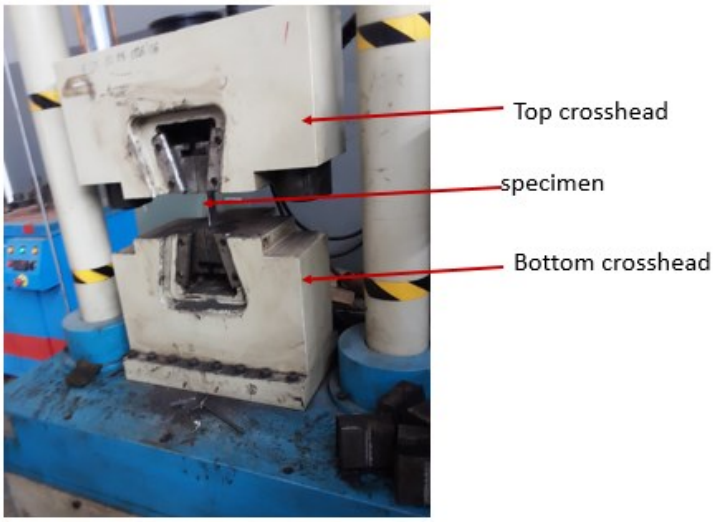

Figure 3.6 The Universal Testing Machine (Ethiopia commodity assessment enterprise)

The computer performs closed-loop control of the various test parameters (load, displacement, and deformation) and permits tests to be carried out at constant increases of any of these physical parameters. The control file is organized as a series of steps (up to 10) to make it easier for the user to generate simple or complex control files or to link several steps together to obtain repeating test sequences. The program also has a control option that allows the user to modify the speed and limits in the file, even during the test

itself. Test-generated data can be examined in separate files, or exported in ASCII format for processing in other programs or databases so that the output can easily be adapted to the user's needs.

The tests are performed on two specimens and the averages are reported in Table 3.2. The average mechanical properties are taken for FEM analysis and other tensile test results are available in Appendix C.

Table 3.2 Experimental result of tensile test

Exp. No	Properties	Units	Tensile test specimens		Average
			1	2	
1	Tensile stress	MPa	122.4	109.8	116.4
2	Elongation	%	16.0	16.3	16.15

The average mechanical properties are taken for FEM analysis and other tensile test results are available in Appendix C.

3.4. Experimental Study on Press Brake Bending Machine

The Experiment has been performed on the hydraulic press brake-bending machine to identify the behavior of sheet metal V-bending process. Bending angles 60°, 90° and 120° are used as of press-brake bending process parameters. The thickness and pitch perforation of materials are used as sheet metal parameters.

3.4.1. Specifications Hydraulic Press Brake Machine (WC67Y-160X3200)

Hydraulic pressure is applied through one or more cylinders to force the ram of the machine down. Due to the hydraulic control of the machine, the ram accuracy is more precisely controlled and adjusted for individual bend depths. Hydraulic machines can have two or four hydraulic cylinders for operation shown in Figure 3.7 and Figure 3.8.

- **Features of WC67Y-160X3200**

- Hydraulic down-stroke construction.
- Synchronizing mechanism of the ram adopting torsion shaft and mechanical stop unit, stable and reliable
- Deflection compensating mechanism of wedge construction.
- Power fast adjustment, manual fine adjustment and counter showing for the ram stroke;
- Back gauge by power fast adjustment and manual fine adjustment with the counter display.

The important specifications of the hydraulic press brake-bending machine are given in Appendix D.

Figure 3.7 Hydraulic Press Brake Machine (WC67Y-160X3200)

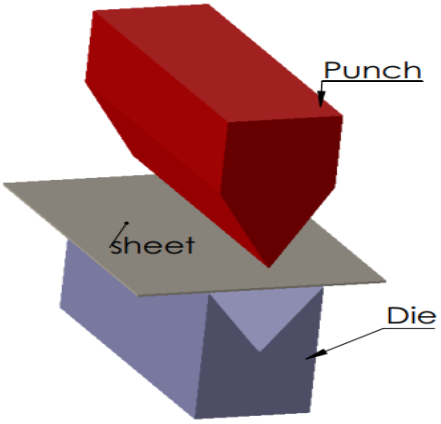

Figure 3.8 Schematic diagram of press brake bending mechanism

3.4.2. Sample Preparation

The v-bending operation performed on aluminum sheets, which are cut into a length of 54 mm and a width of 50 mm with different thicknesses such as 0.5, 1 and 1.5mm using the shearing machine along the transverse (90°). The samples are prepared as plain surface, circular perforated, square perforated and scattered perforated. The perforation performed on the drilling machine.

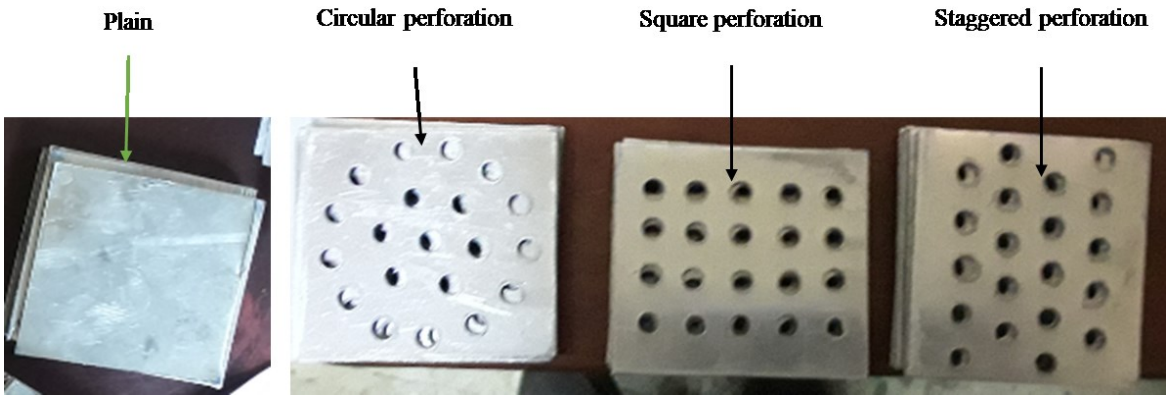

Figure 3.9 Sample prepared for V- bending process

3.4.3. Bending Allowance

The length of the neutral axis in the bend is called bend allowance. The position of the neutral axis depends on the radius and the bend angle. The approximate formula for the bend allowance is given by:

$$L_b = \alpha(R+kT) \qquad 3.1$$

Where

α : Bend angle (in radian).

T: Thickness

R: Bend radius

K: a constant [0.33 (for R<2T) to 0.5 (for R>2T)] (Shariff, Bin, & Awal, 2016)

3.4.4. Bending Parameters

Press brake constant parameters used in the v- bending process are listed in Table 3.3.

Table 3.3 Press-brake constant parameters and considered values

Process parameters	Symbols	Units	Values
Pressure	P	N	16000
Punch radius	R_p	mm	1
Die radius	D_r	mm	2
Corner radii	C_r	mm	1

Its V-bending process parameters (bending angle) and sample parameters (thickness and pitch of perforation) used for numerical and experiments are listed in Table 3.4. Bending allowance calculated according to the equation (3.1).

Table 3.4 Details of press brake v bending analytical process parameters

Exp. No	Thickness w. p (mm)	Types of w. p.	Desired bending Angle (degree)	Depth	Bend allowance (mm)
1	0.5	Circular (C)	60	17.0012	1.220
2	1	Circular (C)	60	17.0012	1.393
3	1.5	Circular (C)	60	17.0012	1.566
4	0.5	Plain (P)	60	17.0012	1.220
5	1	Plain (P)	60	17.0012	1.393
6	1.5	Plain (P)	60	17.0012	1.566
7	0.5	Square (Sq)	60	17.0012	1.220
8	1	Square (Sq)	60	17.0012	1.393
9	1.5	Square (Sq)	60	17.0012	1.566
10	0.5	Staggered (St)	60	17.0012	1.220
11	1	Staggered (St)	60	17.0012	1.393
12	1.5	Staggered (St)	60	17.0012	1.566
13	0.5	Circular (C)	90	13.7574	1.830
14	1	Circular (C)	90	13.7574	2.089
15	1.5	Circular (C)	90	13.7574	2.348
16	0.5	Plain (P)	90	13.7574	1.830
17	1	Plain (P)	90	13.7574	2.089
18	1.5	Plain (P)	90	13.7574	2.348
19	0.5	Square (Sq)	90	13.7574	1.830
20	1	Square (Sq)	90	13.7574	2.089
21	1.5	Square (Sq)	90	13.7574	2.348
22	0.5	Staggered (St)	90	13.7574	1.830
23	1	Staggered (St)	90	13.7574	2.089
24	1.5	Staggered (St)	90	13.7574	2.348
25	0.5	Circular (C)	120	8.3506	2.440
26	1	Circular (C)	120	8.3506	2.786
27	1.5	Circular (C)	120	8.3506	3.131
28	0.5	Plain (P)	120	8.3506	2.440
29	1	Plain (P)	120	8.3506	2.786
30	1.5	Plain (P)	120	8.3506	3.131
31	0.5	Square (Sq)	120	8.3506	2.440
32	1	Square (Sq)	120	8.3506	2.786
33	1.5	Square (Sq)	120	8.3506	3.131
34	0.5	Staggered (St)	120	8.3506	2.440
35	1	Staggered (St)	120	8.3506	2.786
36	1.5	Staggered (St)	120	8.3506	3.131

3.4.5. Procedures of Press Brake Bending

The bending procedures used in the press brake V-bending process according to the following figures. It has changeable tools that used for bending of different angles. Bending allowance calculated based on the thickness of the material and bending angle. The press brake has pressure is 1600kN. Punch radius is 1mm for all angles. Corner radius of the die and die radius is 3mm and 2mm respectively. The timing of bending is based on depth and bending allowance. Figure 3.10 shows different types of punch used in press brake bending machine.

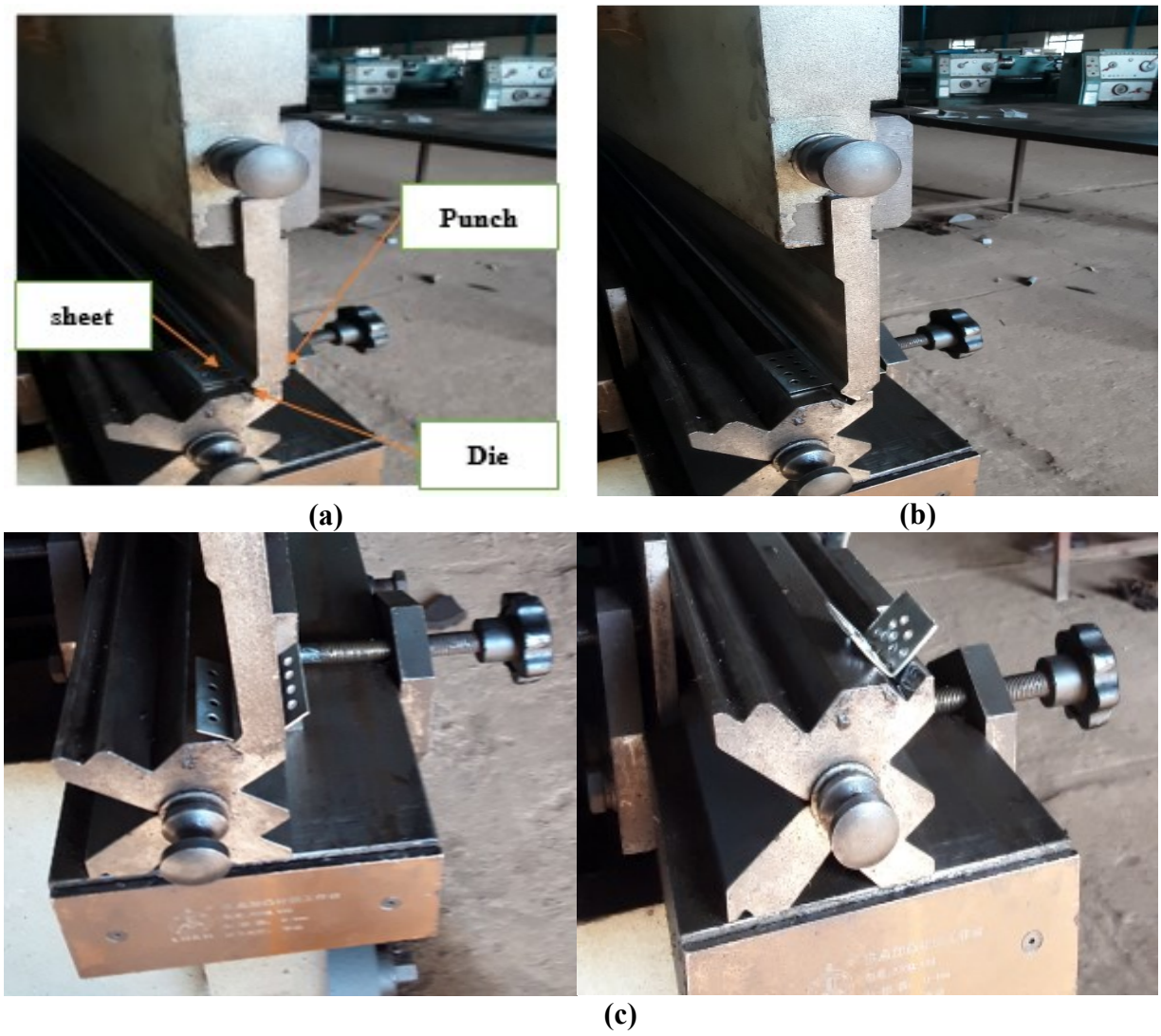

Figure 3.10 Steps of press brake V-bending process (a) first step of bending, (b) unsupported bending and (c) V-bended samples

Figure 3.11 shows different types of die used in press brake bending machine.

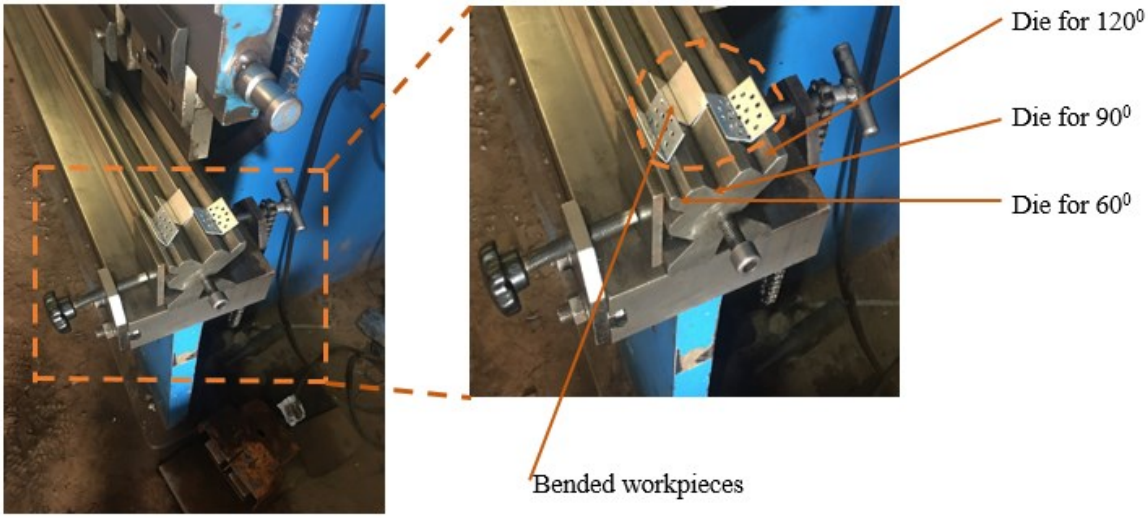

Figure 3.11 Details of press-brake v- bending process workpieces and bend angles.

3.4.6. The Experimental Measure of Spring-back

The bend angle measured using the bevel protractor figure 3.12. Then different repeatedly experimentally measured average of spring-back is compared them with the result of FEM.

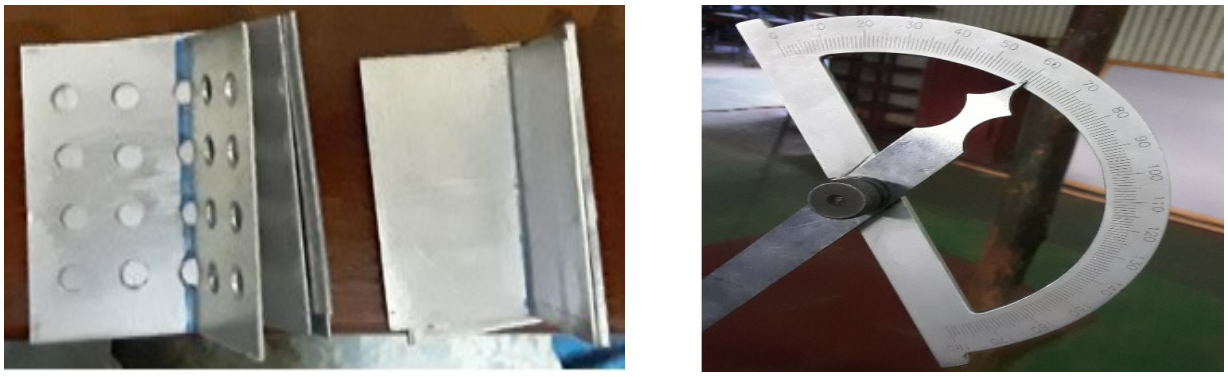

(a) (b)

Figure 3.12 Measuring bend angle of workpieces: (a) bended workpieces and (b) bevel protractor

3.5. FEM Model for Press Brake Bending Process

The commercial FEM package Abaqus/CAE 6.14-5 was used to model the V-bending process using 3D analysis. In Abaqus/CAE modeling process, the following modules were used: part creation, material property, assembly, step, interaction, load, mesh, and job.

3.5.1. Geometry Creation

The geometry is created using Solidwork and CAD geometries for the tools of press-brake according to their parameters. Then imported into Abaqus 6.14-5 using the file format *IGES*, which is designed for the digital exchange of CAD-models between different CAD-systems.

a. Modeling of the die using FEM tools

Die is modeled as Discrete Body-3D Shell. A reference point is created on the Die to specify constraints and boundary conditions for the Die, which is meshed with the 4-node 3-D bilinear rigid quadrilateral element (R3D4).

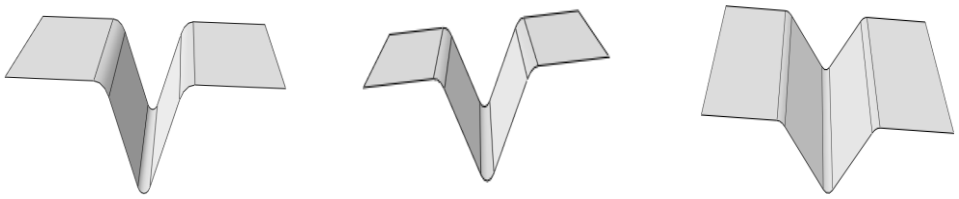

(a) (b) (a)

Figure 3.13 3D model of the Die modeled as Discrete Rigid Body-3D in the FE tool (a) Die of the v bending 60^0 (b) Die of the v bending 90^0 and (c) Die of the v bending for 120^0

b. Modeling of Punch

Punch is also modeled as Discrete Body-3D Shell. A reference point is created on the punch to specify constraints and boundary conditions for the Punch, which is meshed using 4-node 3-D bilinear rigid quadrilateral (R3D4).

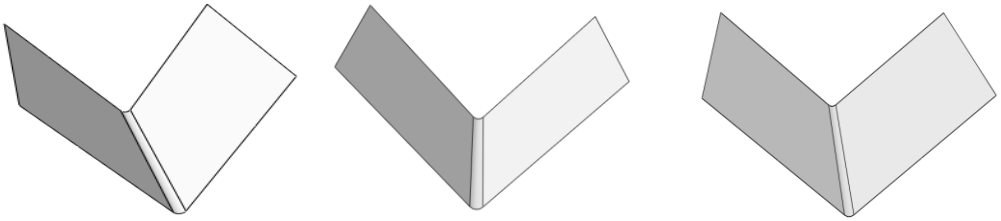

(a) (b) (c)

Figure 3.14 3D models of the Punch modeled as Discrete Rigid Body-3D Shell (a) the punch of the v bending for 60° (b) The punch of the v bending for 90° and (c) The punch of the v-bending for 120°

c. Modeling of Sheet

The sheet is modeled with a 3D Deformable-body with the extruded shell-mid surface with a uniform shell thickness of 0.5, 1 and 1.5mm. Figure 3.7 shows three different parts geometry such as plain, square and staggered perforated are modeled for the experiment. The sheet has meshed with brick element C3D8R. With a 4- node doubly curved thin or thick shell, reduced integration, hourglass control, finite membrane strains.

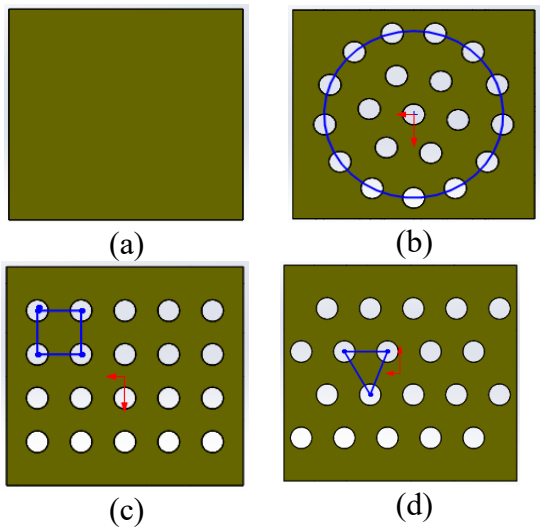

Figure 3.15 3D models of Sheet modeled as 3D Deformable Extruded Sheet-mid surface (a) Plain Sheet (b) Circular Perforated Sheet (c) Square Perforated Sheet and (d) Staggered Perforated Sheet

3.5.2. Material Properties Definition

Material property definition for discrete rigid bodies i.e. for die and punch is not required, as they are considered as rigid. Material property for a Deformable sheet is defined as the nonlinear material. Important properties are inserted from the tensile test values of the testing machine.

3.5.3. Assembly of Die, Punch, and Sheet

Initially, the die punch and sheet are assembled in a position as shown in Fig 3.8 Meshed model of the assembly is shown in Fig. 14.

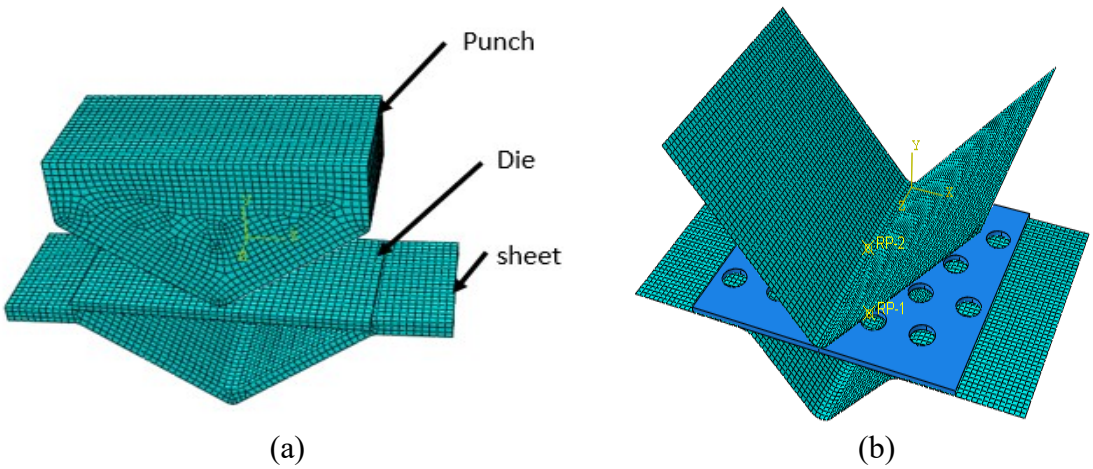

Figure 3.16 FE model of Assembly of the Die Punch Set in Abaqus: (a) meshed sheet material and (b) meshed punch and die

3.5.4. Boundary Conditions

a. Interaction or Contact definition

Surface to surface contact with finite sliding conditions is defined between the sheet and Die and for die and punch. Initially, the sheet is resting on the die i.e. they are just touching each other and punch is in contact with the sheet.

b. Displacement Boundary condition

Die is kept fixed. Displacement boundary conditions are given for the punch in the number of steps. Punch moves gradually towards down and bend the sheet. Once the die comes to its lowest extreme, position the sheet takes the outer shape of the punch/die. Immediately after that, the punch is displaced upward and the final deformed shape of the sheet is obtained.

The v-bending process involves nonlinear interaction between various press brake parameters and workpieces geometry parameters. The following assumptions were considered in the simulation:

- The material is isotropic and solid homogeneous.
- The change of thickness during bending is ignored.
- The von- Mises yield criterion is used.
- Friction is negligible (Panthi et al. 2010) (Trzepiecinski and Lemu 2017).

3.6. Measurement of Spring-back using FEM

Press brake bending quality is one of the major expectations in v-bending processes. Different process parameters in press-brake bending play a crucial role in providing better quality results. After a bending operation, residual stresses will cause the sheet metal to spring-back slightly due to elastic recovery. This elastic recovery is called spring-back.

(Choudhury & Ghomi, 2014) The spring-back is the difference between the bent angle after the removal of load and the die angle.

$$\text{Spring-back} = \phi_f - \phi_i \tag{3.2}$$

The percentage spring-back angle is calculated as:

$$\%\,\text{spring-back} = \frac{\text{spring-back}}{\text{die angle}} \times 100 \tag{3.3}$$

The spring-back of the sheet is calculated by Abaqus/implicit when deformation simulation of Abaqus/explicit is terminated (Cui et al. 2019). The measurement spring-back using FEM is by taking the node distance of deformed 3D deformed sheet metal. Then the distance node of three-point is drawn and measure on a new window of Abaqus/CAE Figure 3.17.

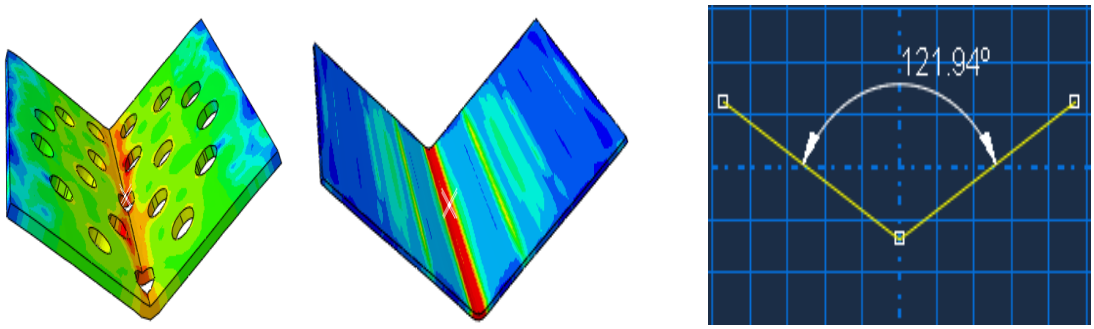

(a) (b)

Figure 3.17 Measurement of spring-back using FEM: (a) 3D bended sheet metal and (b) measured angle

3.7. Mesh Sensitivity

Numerical simulations of press brake v bending processes are performed to determine spring-back. the element used for mesh is 3D brick elements (C3D8R) for the deformable models, and rigid discrete elements (R3D4) are selected for discrete rigid tools (Zhang et al.2018). As illustrated in Table 3.5, the mesh sensitivity study was carried out by varying mesh sizes and comparing the simulation time with the bend angle for press brake load 1600KN, the width samples are 54mm x 50 mm.

Table 3.5 Mesh sensitivity study for fine mesh region workpieces size (L × w × 1.5) mm.

Thickness of workpieces(mm)	Element size (mm^3)	Bend angle (degree)	Screen time (s)
1.5	2.5 × 1 × 2.4545	121.72	205
	2 × 1 × 1.928	121.36	248
	1.5 × 1 × 1.5152	121.12	294
	1 × 1 × 0.75	**121.93**	**445**
	0.75 × 0.75 × 0.746	121.90	503

After the mesh sensitivity study for a 120° bend angle, the element of size 0.5 mm x 1mm x 0.75

mm was chosen for the 1.5mm thickness. It concluded that two elemental divisions were taken in the thickness direction for 0.5mm, 1mm and 1.5 (mm) thickness for all bending angles .and its appropriateness was confirmed by the mesh sensitivity analysis.

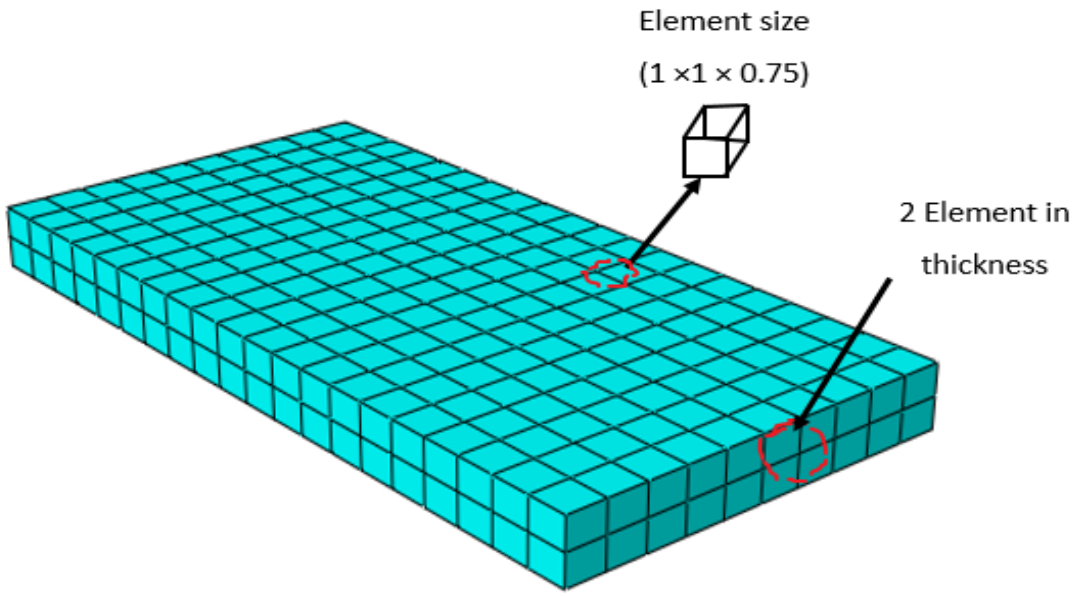

Figure 3.18 Element size of mesh sensitivity

Chapter- Four

4. Results and Discussion

4.1.Introduction

This chapter presents numerical and experimental studies on press brake bending of the v bending process. Initially, the methodology for numerical simulations using the finite element method is presented. Further, the detailed analysis of the effects of process parameters on the press brake v bending process mechanism and spring-back is discussed. The experiments were carried out to validate the results predicted by the numerical model. In this chapter, the effect of process parameters *viz.*, workpieces thickness, bend angle, and pitch of perforation is discussed.

4.2.Procedures of Experiments and FEM Simulation

Numerical simulations were carried out using Abaqus/CAE 6.14-5 package in order to analyze the variations in the bend angle by using a press brake-bending machine with different parameters. Details regarding the boundary conditions and mesh sensitivity were discussed in Chapter 3. Based on number of simulations carried out the appropriate parameters of the press-brake, the v-bending process selected. The bending allowance and depth of bending selected in the experiments. Details of experiments, such as experimental machine, sample preparation, bend angle methodology and procedure measurement were presented in Chapter 3. V-bending process bending performed by using press brake bending machine.

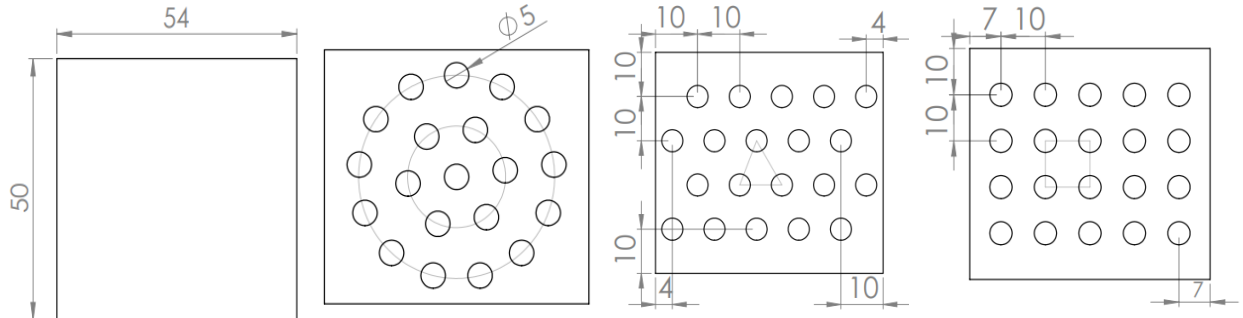

Figure 4.1 The workpieces for the v-bending process with the size of $54mm \times 50mm$ with the thickness $0.5mm, 1mm$ and $1.5mm$ (a) plain (b) circular perforated (c) staggered perforated and (d) square perforated

4.2.1.Validation of FEM

The validation of numerical results with experiments is performed on plain and staggered perforated AA. The parameters used for the press-brake bending process are discussed in chapter 3. The numerical simulation results for the bend angle were compared with experimental results to verify the validity of the numerical simulation. Table 4-1 and Table 4-2 shows the percentage deviation between experimental and numerical simulation results for plain and staggered perforated bending angle at 60° and 90°. A maximum deviation is 17.2% is observed for the experiment.

Table 4.1 Experimental and simulated bend angle of plain AA1300

Exp. & FEM Parameters				**Response**					
Exp. No	**Thickness w. p (mm)**	**Types of w. p**	**Desired Bending angle (degree)**	**Exp. Spring-back(degree)**				**FEM Spring-back (degree)**	**Error (%)**
				Exp.1	**Exp.2**	**Exp.3**	**Avg.**		
1	0.5	p	60	4.5	4	5	4.5	4.70	9.5
2	1	p	60	4	3	3.5	3.5	3.90	2.5
3	1.5	p	60	3	3	3	3	3.80	2.6
4	0.5	p	90	3.5	4.5	4	4	3.90	-2.5
5	1	p	90	4	3.5	3	3.5	3.42	2.28
6	1.5	p	90	2	3	2.5	2.5	2.93	17.2

P. – Plain, Exp. – Experiments, Avg. – Average, w. p. – workpieces

Table 4.2 Experimental and simulated bend angle of staggered perforated AA1300

Exp. & FEM Parameters				**Response**					
Exp. No	**Thickness w. p (mm)**	**Types of w. p.**	**Desired bending Angle (degree)**	**FEM Spring-back (degree)**	**Exp. Spring-back (degree)**				**Error (%)**
					Exp.1	**Exp.2**	**Exp.3**	**Avg.**	
1	0.5	St. PP	60	4.49	4	3.5	4.5	4	4.75
2	1	St. PP	60	3.82	3.5	4	3	3.5	6.28
3	1.5	St. PP	60	3.41	2.5	3.5	3	3	7
4	0.5	St. PP	90	4.04	4	4	4	4	1
5	1	St. PP	90	3.51	3	4	3.5	3.5	0.28
6	1.5	St. PP	90	3.02	3	3	3	3	0.6

St. PP.-Staggered Pitch of Perforated, Exp. – Experiments, w. p. – workpieces

a. Bending angle @60°

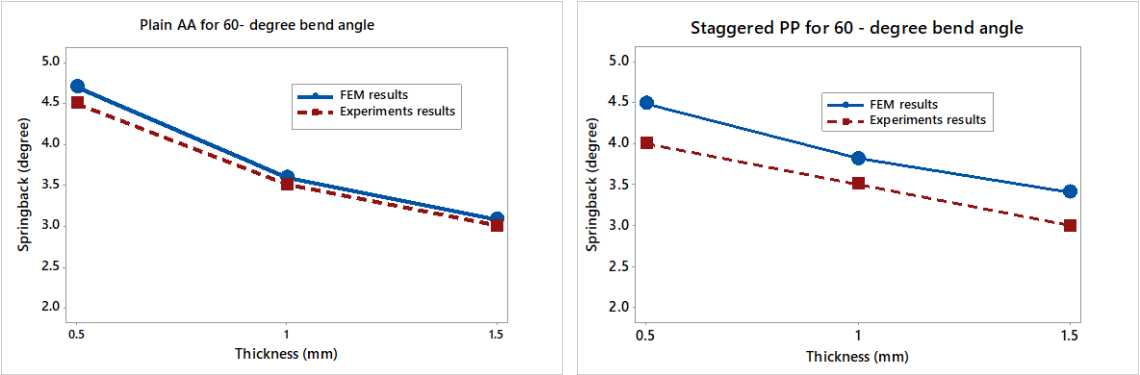

(a) (b)

Figure 4.2 Comparison between experimental and simulation results for a 60° bend angle for plain and staggered perforated AA1300.

Fig. 4.2 shows the bend angle deviation of experimental and simulation results for the plain and staggered pitch of perforation of blanks bend angle at 60°. The staggered pitch of perforation value experiments and simulations is closest to each other than plain samples. The spring-back is decreasing as the thickness increase.

b. Bending angle @90°

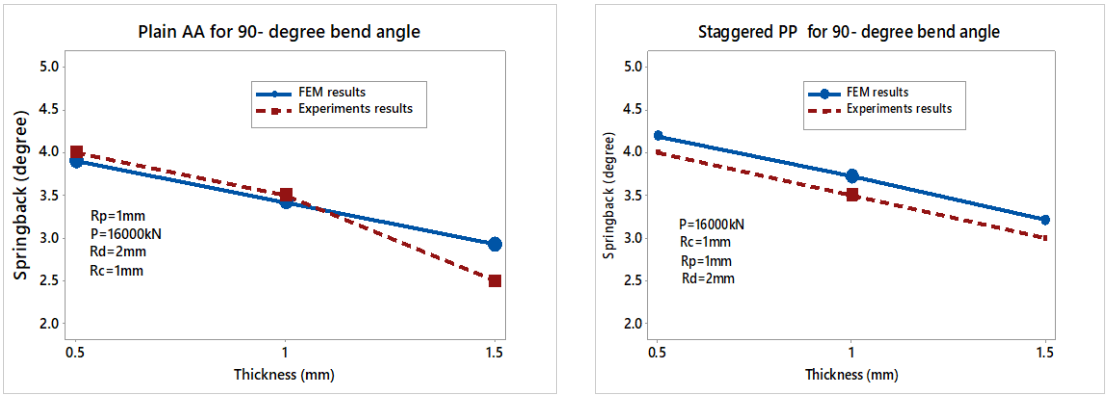

(a) (b)

Figure 4.3 Comparison between experimental and simulation results for a 90° bend angle for plain and staggered perforated AA1300.

Fig. 4.2 and 4.3 show that, the spring-back is decreasing along with increasing the thickness. However, the percentage variations are very small for the plain and staggered pitch of the perforation bend angle at a 60° and 90° bending angle. It is observed that the experimental results have a good agreement with the simulated ones.

4.3. Results of Numerical Studies

The behavior of material components under the press-brake of the v-bending process was influenced by combinations of press bending process parameters, geometry, and material parameters. In this work, the effect of process parameters, such as bending angle, workpieces thickness, and Pitch of perforation on the spring-back is presented based on FEM results.

4.3.1. Effect of Thickness of Materials

The simulations are conducted to study the effect of process parameters such as sheet thickness, the pitch of perforation and bend angle in the press-brake v-bending process of AA1300. The thickness of blank material is selected as 0.5mm, 1mm and 1.5mm. Bend angle is selected 60°, 90°, and 120°.

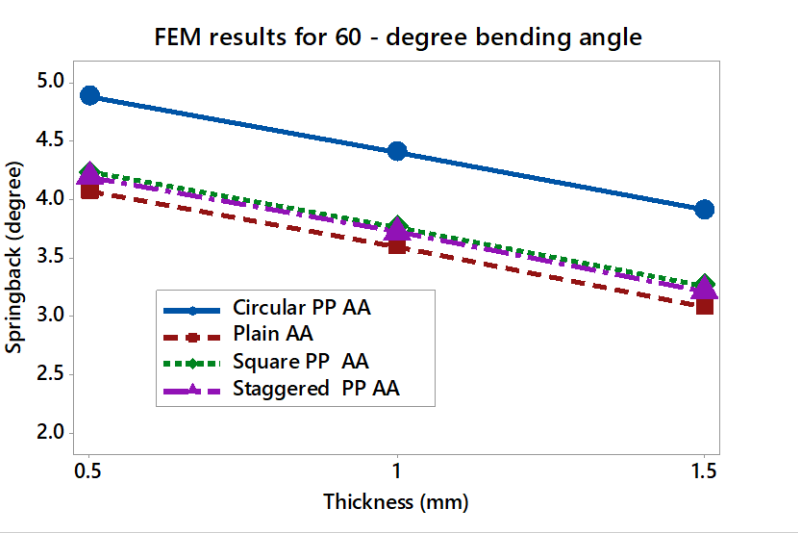

Figure 4.4 Variation of spring-back with different thicknesses for a 60° bend angle

Figure 4.8 shows simulation is done with the 60° bending angle on the AA1300 of thickness 0.5mm, 1mm, and 1.5mm. The spring-back v/s thickness graph shows that there is a decrement in spring-back value with the increments of thickness. The spring-back is higher for the 0.5mm thickness of the sheet. Spring-back of sheets with holes arranged in the circular pitch of perforation is more than that of other blanks. Sheet with the square pitch of perforation has more spring-back next to circular perforation. Plain sheets have smaller spring-back. Except for the circular perforated sheet, the spring-back other perforated sheet is all closest to each other.

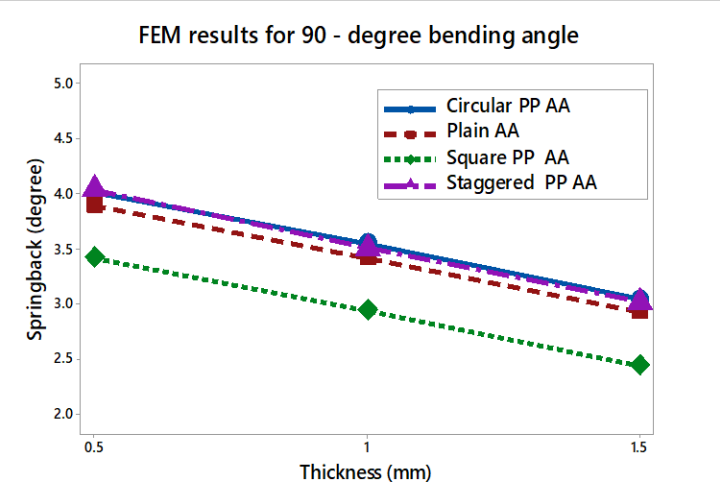

Figure 4.5 Variation of spring-back with different thicknesses for a 90° bend angle.

Figure 4.5 Shows simulation is done with the 90° bending angle on the AA1300 of thickness 0.5mm, 1mm, and 1.5mm. The spring-back v/s thickness graph shows that there is an increment in spring-back value as thickness increases. The spring-back for a 90° bend angle is lower than that of for 60° bend angle. The spring-back is a small variation for different types of samples.

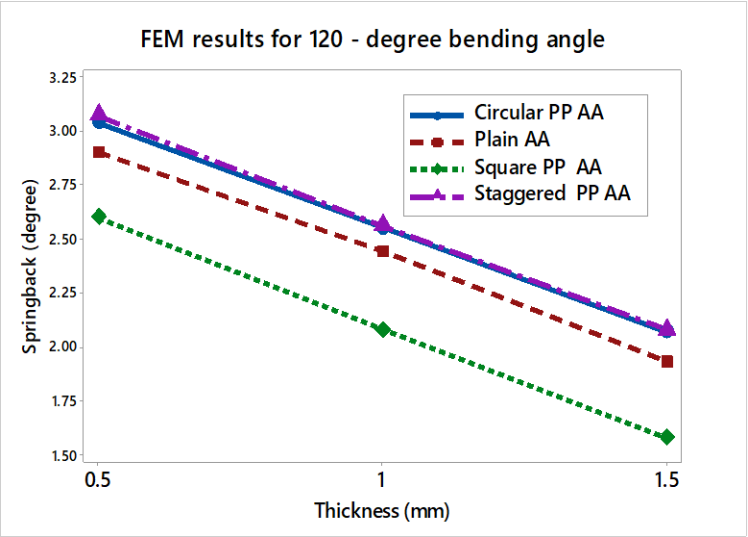

Figure 4.6 Variation of spring-back with different thickness for 120° bend angle

Figure 4.6 shows simulation is done with the 120° bending angle on the AA1300 of thickness 0.5mm, 1mm, and 1.5mm. The spring-back is decreasing with increasing thickness of the material. The spring-back value for the circular and staggered perforated sample has the closest spring-back value. The square pitch of perforation has small spring-back values. Spring-back decreases with the increase of thickness of samples. Within the increase of the bending angle, the circular pitch perforation spring-back close to other perforated blanks.

4.3.2. Effect of Bending Angle

The bending angle is an important parameter that directly controls the spring-back of the workpieces. The spring-back decreases with the decreasing of bending angle. The simulation and experimental results revealed that the spring-back was critically dependent on the bending angle. It was observed that the numerical results were in good agreement with the experimental results. The trend of variation of the bend angle predicted by the developed numerical model was similar to those obtained in the experiment.

Figure 4.4 shows that 0.5mm thickness AA1300 bent at a different angle. The spring-back decreases with the increasing of bend angle. The spring-back for the circular PP higher angle for bend angle between 60° and 90°. Staggered PP has higher spring-back for bend angle between 60° and 90°. Square PP has lower spring-back.

Figure 4.5 shows that 1mm thickness AA1300 bent at a different angle. The spring-back decreases from 60° to 120° of bending angle. The spring-back for the circular PP has a higher angle than plain and differently perforated PP. The perforated surface has a different spring-back for the different bending angles. Spring-back is higher for staggered PP next to circular PP.

Figure 4.6 shows that 1.5mm thickness AA1300 bent at a different angle. The different samples have different spring-back for the different bending angles. Spring-back decreases with the increase of bending angle. The spring-back smoothly decreasing from 90° and 120°. The spring-back for all samples are close to each other except square PP.

Out of all the 36 simulations carried out for plain sheet metal and perforated sheet metal, it is observed that a minimum spring-back value of 2.60°,2.08° and 1.58° is generated for square pitch perforated sheet of 0.5mm,1mm and 1.5mm thickness during the bending process at 120° bending angle respectively. Maximum spring-back value observed 4.88°, 4.40° and 3.91° is generated for circular pitch perforated sheet 0.5mm,1mm and 1.5mm thickness during the bending process at 60° bending angle respectively.

Chapter-Five

5. Optimization

5.1 Multi-Objective Optimization

The selection of techniques is to be done based on the number of process variables, so hence it is noted that there are three process parameters *viz.* blank thickness, bending angle, the pitch of perforation and spring back values experimental or FEM simulations. Therefore, Weighted Principal Component (WPC) used as an optimization technique. Larger MPI (Multi-response performance index) value shows optimum results (Jayakumar, 2017). The steps of Multi-objective optimization as follows:

5.1.1. Signal to Noise Ratio (S/N)

A larger S/N ratio represents better quality characteristics because of the minimization of noise. Following steps to follow for the WPC method:

$$\frac{S}{N} = -10\log\left(\frac{1}{n}\sum_{i=1}^{n} y^2 i\right) \qquad (5.1)$$

Where, n = number of experiment

y = out put

Based on the stress values obtained from different simulations, S/N ratio values have to be calculated for AA1300 materials circular pattern with rectangular, triangular and Staggered Pattern.

S/N ratio values for a plain AA1300 tabulated shown in Table 5.1.

Table 5.1 S/N Ratio values derived for circular pitch perforated AA1300

Exp. No	Thickness (mm)	Bending angle (degree)	Spring-back (degree)	S/N Ratio
1	0.5	60	4.88	-13.76
2	1	60	4.40	-12.86
3	1.5	60	3.91	-11.84
4	0.5	90	4.01	-12.06
5	1	90	3.55	-11.00
6	1.5	90	3.04	-9.65
7	0.5	120	3.04	-9.65
8	1	120	2.55	-8.13
9	1.5	120	2.07	-6.31

S/N ratio values for the circular perforated AA1300 tabulated shown in Table 5.2.

Table 5.2 S/N Ratio values derived for plain AA1300

Exp. No	Thickness (mm)	Bending angle (degree)	Spring-back (degree)	S/N Ratio
1	0.5	60	4.70	-13.44
2	1	60	3.90	-11.82
3	1.5	60	3.80	-11.59
4	0.5	90	3.90	-11.82
5	1	90	3.42	-10.68
6	1.5	90	2.93	-9.33
7	0.5	120	2.90	-9.24
8	1	120	2.44	-7.74
9	1.5	120	1.93	-5.74

S/N ratio values for the square perforated AA1300 tabulated shown in Table 5.3.

Table 5.3 S/N Ratio values derived for square perforated AA1300

Exp. No	Thickness (mm)	Bending angle (degree)	Spring-back (degree)	S/N Ratio
1	0.5	60	4.23	-12.52
2	1	60	3.76	-11.50
3	1.5	60	3.26	-10.26
4	0.5	90	3.42	-10.68
5	1	90	2.94	-9.36
6	1.5	90	2.44	-7.74
7	0.5	120	2.60	-8.29
8	1	120	2.08	-6.36
9	1.5	120	1.58	-3.97

S/N ratio values for the square perforated AA1300 shown in Table 5.4.

Table 5.4 S/N Ratio values derived for staggered perforated AA1300

Exp. No	Thickness (mm)	Bending angle (degree)	Spring-back (degree)	S/N Ratio
1	0.5	60	4.49	-13.04
2	1	60	3.82	-11.64
3	1.5	60	3.41	-10.65
4	0.5	90	4.04	-12.12
5	1	90	3.51	-10.90
6	1.5	90	3.02	-9.60
7	0.5	120	3.07	-9.74
8	1	120	2.56	-8.16
9	1.5	120	2.08	-6.36

5.1.2. Original Multi Response Array m Number of Test Trials and n Number of Responses

$$X = \begin{bmatrix} X_1(1) & X_1(2) & . & . & X_1(n) \\ X_2(1) & X_2(2) & . & . & X_2(n) \\ X_3(1) & X_3(2) & . & . & X_3(n) \\ . & . & . & . & . \\ . & . & . & . & . \\ X_m(1) & X_m(2) & . & . & X_m(n) \end{bmatrix} \quad (5.2)$$

Where

x = S/N ratio of response

m = number of test trials

n = number of responses

$$X_1 = \begin{bmatrix} -13.76 \\ -12.86 \\ -11.84 \\ -12.06 \\ -11.00 \\ -9.65 \\ -9.65 \\ -8.13 \\ -6.31 \end{bmatrix}, X_2 = \begin{bmatrix} -13.44 \\ -11.82 \\ -11.59 \\ -11.82 \\ -10.68 \\ -9.33 \\ -9.24 \\ -7.74 \\ -5.74 \end{bmatrix}, X_3 = \begin{bmatrix} -12.52 \\ -11.50 \\ -10.26 \\ -10.68 \\ -9.36 \\ -7.74 \\ -8.29 \\ -6.36 \\ -3.97 \end{bmatrix} \text{ and } X_4 = \begin{bmatrix} -13.04 \\ -11.64 \\ -10.65 \\ -12.12 \\ -10.90 \\ -9.60 \\ -9.74 \\ -8.16 \\ -6.36 \end{bmatrix}$$

Where:

X_1 = Circular pattern perforated

X_2 = Plain

X_3 = Square pattern perforated

X_4 = Staggered pattern perforated

5.1.3. **Normalized S/N Ratio**

The formula used for deriving the values for Normalized S/N Ratio mentioned below.

$$X_i^*(j) = \frac{x_i(j) - x_i(j)\min}{x_i(j)\max - x_i(j)\min} \tag{5.3}$$

Where: x_i^* = normalized value of the response,

$(x_i(j)\min)$ and $(x_i(j)\max)$ is the minimum and maximum of $(x_i(j))$ respectively.

j =1,2,3.....m

The normalized multi-response array X^* can be expressed as,

$$X^* = \begin{bmatrix} x_1^*(1) & x_1^*(2) & . & . & x_1^*(n) \\ x_2^*(1) & x_2^*(2) & . & . & x_2^*(n) \\ x_3^*(1) & x_3^*(2) & . & . & x_3^*(n) \\ . & . & . & . & . \\ . & . & . & . & . \\ x_m^*(1) & x_m^*(2) & . & . & x_m^*(n) \end{bmatrix} \tag{5.4}$$

$$x_1^* = \begin{bmatrix} 0.00 \\ 0.12 \\ 0.26 \\ 0.23 \\ 0.34 \\ 0.55 \\ 0.55 \\ 0.75 \\ 1.00 \end{bmatrix}, x_2^* = \begin{bmatrix} 0.00 \\ 0.21 \\ 0.24 \\ 0.21 \\ 0.36 \\ 0.53 \\ 0.54 \\ 0.74 \\ 1.00 \end{bmatrix} x_3^* = \begin{bmatrix} 0.00 \\ 0.12 \\ 0.26 \\ 0.21 \\ 0.37 \\ 0.56 \\ 0.49 \\ 0.72 \\ 1.00 \end{bmatrix} \text{ and } x_4^* = \begin{bmatrix} 0.00 \\ 0.21 \\ 0.36 \\ 0.14 \\ 0.32 \\ 0.51 \\ 0.49 \\ 0.73 \\ 1.00 \end{bmatrix}$$

Where

x_1^* = Circular pattern perforated

x_2^* = Plain

x_3^* = Square pattern perforated

x_4^* = Staggered pattern perforated

5.1.4. The Calculation for Eigen Values, Eigen Vectors, and Covariance Matrix.

a. For circular perforated AA1300

The covariance matrix is calculated using MATLAB.

$$A = \mathrm{cov}\left(x_1^*\right) \tag{5.5}$$

$$A = \begin{bmatrix} 0.1017 & 0 \\ 0 & 0 \end{bmatrix}$$

Using equation,

$$[A-\lambda I]*[V]$$

Principal component	Eigenvalue	The proportion of explained variation	Eigenvector
Frist	0	0.1017	$[0 \quad 0]$
Second	0.1017	0	$[0 \quad 0.1017]$

b. For plain AA1300

The covariance matrix is calculated using MATLAB.

Principal component	*Eigenvalue*	*The proportion of explained variation*	*Eigenvector*
Frist	0	0.0957	$[0 \quad 0]$
Second	0.0957	0	$[0 \quad 0.0957]$

c. For square AA1300

The covariance matrix is calculated using MATLAB.

Principal component	*Eigenvalue*	*The proportion of explained variation*	*Eigenvector*
Frist	0	0.0987	$[0 \quad 0]$
Second	0.0987	0	$[0 \quad 0.0987]$

d. For staggered AA1300

The covariance matrix is calculated using MATLAB.

Principal component	*Eigenvalue*	*The proportion of explained variation*	*Eigenvector*
Frist	0	0.0947	$[0 \quad 0]$
Second	0.0947	0	$[0 \quad 0.0947]$

5.1.5. Principal Component Matrix

The common equation used in deriving the principal Component Matrix(Y) is mentioned below:

$$Y_{m,n} = \sum_{i=1}^{n} x^{*}_{m,n} v_{n,n} \tag{5.6}$$

$$Y_1 = \begin{bmatrix} 0.0000 \\ 0.0122 \\ 0.0264 \\ 0.0233 \\ 0.0345 \\ 0.0559 \\ 0.0559 \\ 0.0762 \\ 0.1017 \end{bmatrix}, Y_2 = \begin{bmatrix} 0.0000 \\ 0.0200 \\ 0.0229 \\ 0.0200 \\ 0.0344 \\ 0.0507 \\ 0.0516 \\ 0.0708 \\ 0.0957 \end{bmatrix}, Y_3 = \begin{bmatrix} 0.0000 \\ 0.0118 \\ 0.0256 \\ 0.0207 \\ 0.0365 \\ 0.0552 \\ 0.0483 \\ 0.0710 \\ 0.0987 \end{bmatrix} \text{ and } Y_4 = \begin{bmatrix} 0.0000 \\ 0.0198 \\ 0.0340 \\ 0.0132 \\ 0.0303 \\ 0.0482 \\ 0.0464 \\ 0.0691 \\ 0.0949 \end{bmatrix}$$

Where:

V = Eigen vector

Y_1 = Circular pattern perforated

Y_2 = plain

Y_3 = Square pattern perforated

Y_4 = Staggered pattern perforated

5.1.6. Evaluating the principal components

$$W_K = \frac{\lambda_K}{n}, \text{ k = 1, 2...n} \tag{5.7}$$

Where:

W_K = weight of the principal component and

λ_k = Eigen values.

K= number of experiments

5.2.6. Multi Response Performance Index (MPI)

Multi response performance index (MPI) is calculated for j^{th} a trial using the formula,

$$\mathrm{MPI_j} = \sum_{i=1}^{n} \mathrm{W_i} \times \mathrm{Y_{ij}} \tag{5.8}$$

Final values for MPI for plain AA1300 are shown in Table 5.5.

Table 5.5 MPI values derived for circular pitch perforated AA1300

Exp. No	Thickness (mm)	Bending angle (degree)	Spring-back (degree)	MPI value
1	0.5	60	4.88	0.000000
2	1	60	4.40	0.000148
3	1.5	60	3.91	0.000696
4	0.5	90	4.01	0.000542
5	1	90	3.55	0.001190
6	1.5	90	3.04	0.003124
7	0.5	120	3.04	0.003124
8	1	120	2.55	0.005806
9	1.5	120	2.07	0.010342

Final values for MPI for plain AA1300 are shown in Table 5.6.

Table 5.6 MPI values derived for plain AA1300

Exp. No	Thickness (mm)	Bending angle (degree)	Spring-back (degree)	MPI value
1	0.5	60	4.70	0.000000
2	1	60	3.90	0.000400
3	1.5	60	3.80	0.000524
4	0.5	90	3.90	0.000400
5	1	90	3.42	0.001183
6	1.5	90	2.93	0.002570
7	0.5	120	2.90	0.002662
8	1	120	2.44	0.005012
9	1.5	120	1.93	0.009158

Final values for MPI for square pattern perforated AA1300 are shown in Table 5.7.

Table 5.7 MPI values derived for square pattern perforated AA1300

Exp. No	Thickness (mm)	Bending angle (degree)	Spring-back (degree)	MPI value
1	0.5	60	4.23	0.000000
2	1	60	3.76	0.000139
3	1.5	60	3.26	0.000655
4	0.5	90	3.42	0.000428
5	1	90	2.94	0.001332
6	1.5	90	2.44	0.003047
7	0.5	120	2.60	0.002332
8	1	120	2.08	0.005031
9	1.5	120	1.58	0.009741

Final values for MPI for staggered pattern perforated AA1300 are shown in Table 5.8.

Table 5.8 MPI values derived for staggered pattern perforated AA1300

Exp. No	Thickness (mm)	Bending angle (degree)	Spring-back (degree)	MPI value
1	0.5	60	4.49	0.000000
2	1	60	3.82	0.000392
3	1.5	60	3.41	0.001156
4	0.5	90	4.04	0.000174
5	1	90	3.51	0.000918
6	1.5	90	3.02	0.002323
7	0.5	120	3.07	0.002152
8	1	120	2.56	0.004774
9	1.5	120	2.08	0.009006

The following graph prepared using all the above formulas as per the WPC technique. The process parameters can be obtained having the largest MPI Values in order to optimize the spring-back value observed at the bending angle. The figures with final MPI Values for all the Plain and perforated sheets of AA1300 are shown in the graph below.

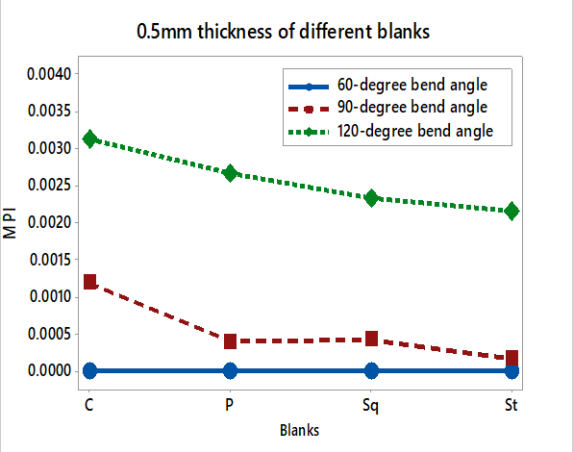

Figure 5.1 Final values for MPI for different types of the workpieces for 0.5mm thickness

The Figure 5.1 shows the optimal parameters for a 60° bend angle of 0.5mm thickness samples are optimum for all samples having the same MPI value. Circular pitch perforation of 0.5mm thickness having the largest MPI value of 1.2×10^{-3} is optimal parameters for a 90° bend angle. Circular pitch perforation of 0.5mm thickness having the largest MPI value of 3.12×10^{-3} is optimal parameters for a 120° bend angle.

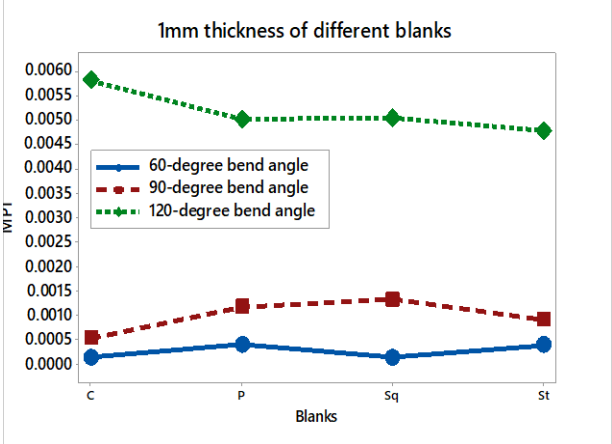

Figure 5.2 Final values for MPI for different types of the workpieces for 1mm thickness

The Figure 5.2 shows plain samples of 1mm thickness having the largest MPI value 4×10^{-3} is optimal parameters for 60° bend angle. Square pitch perforation of 1mm thickness having the largest MPI value 1.33×10^{-3} it is optimal parameters for 90° bend angle. Circular pitch perforation of 1mm thickness having the largest MPI value 5.8×10^{-3} it is it is optimal parameters for 120° bend angle.

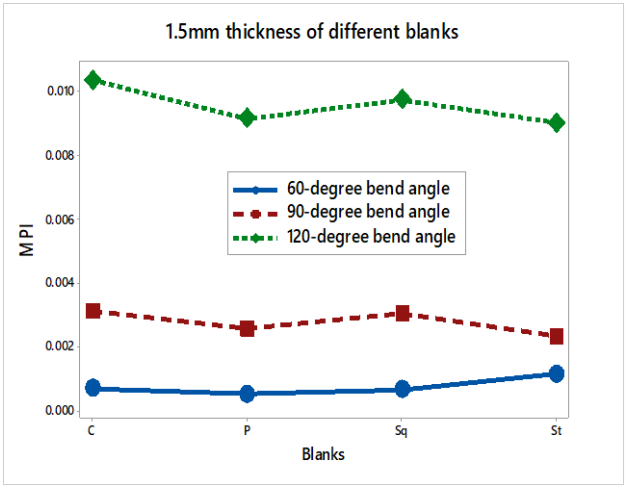

Figure 5.3 Final values for MPI for different types of the workpieces for 1.5mm thickness

The Figure 5.1 shows that staggered pitch perforation of 1.5mm thickness having the largest MPI value 1.16×10^{-3} is optimal parameters for 60° bend angle. Circular pitch of perforation of 1.5mm thickness of the sheet are a having the largest MPI value 3.12×10^{-3} is optimal parameters for a 90° bend angle. Circular pitch of perforation of 1.5mm thickness of having the largest MPI value 10.34×10^{-3} is optimal parameters for a 120° bend angle.

Chapter-Six

6. Conclusion and Scope for Future Work

6.1. Conclusion

This research was carried out on selective cases for Plain and Perforated Sheet metal. It has been proved that numerical simulations can predict the same results as experimental results for different samples. Conducted experimental, numerical simulations and parametric optimization of press brake bending process of AA1300 concluded that:

- The FEM simulation compared with experiments with permissible limits and it is observed that the experimental results have a good agreement with the simulated ones.
- The spring-back is a function of material thickness, bending angle and perforation of materials. For different parameters, the spring-back for the parts with less thickness is greater than the parts with more thickness.
- The influence of the perforation of on the spring-back in the 60° bending angle is greater than that in the 90° bending angle, and the influence of the 90° bending angle is greater than that in the 120° bending angle.
- Perforation has an influence on the formability of AA1300. Plain and perforated sheets metals have different spring-back. The spring-back of the circular perforated sheet metals are nearly greater than that of the plain. The spring-back of the square perforated sheet AA, are almost lower spring back than plain and other type of perforated AA.
- The pitch of perforation of the bending surface has an effect on the spring-back. When the pitch of perforation is square, smaller spring-back is observed. When the pitch of perforation is circular, larger spring-back is observed.
- The effects of perforations depended on the thickness of the material and bending angle.
- The thickness of materials is an important parameter in perforated components bending operations. When it is decreased, the spring-back is increased.
- The bending angle is an important parameter in perforated components bending operations. When that is increased, the spring-back is decreased.
- Press-brake can produce a good quality of AA1300 by the v-bending process.
- Process parameters of 60° bend angle are optimum for 0.5mm thickness for all samples AA1300. It is optimum for 1mm thickness for plain AA1300 and optimum for 1.5mm

thickness for staggered pitch of perforation.

- Process parameters of 90° bend angle are optimum for circular pitch of perforation for 0.5mm, 1mm and 1.5mm thickness AA.
- Process parameters of 120° bend angle are optimum for circular pitch of perforation for 0.5mm, 1mm and 1.5mm thickness AA.

6.2. Recommendation for Future Work

- This work has investigated spring-back on the press-brake v-bending process of on same material. The work can be extended to dissimilar materials.
- There is a need to carry out more experimental and numerical investigations on the metallurgical aspects of the bent area.
- The present work related to the spring-back effect of the size of the same hole of circle perforation. The work can extend to different hole size perforation.
- The present work related to constant parameters of the press-brake bending angle. The work can extend to different process variables such as punch radius, die radius and depth of bending.
- The present work related to the perforated sheet metals bending process. The work can extend to perforate plate bending.
- The present work based on the transverses direction of material. The work can extend to transverses direction of material.

7. References

- *[Robert_Creese]_Introduction_to_Manufacturing_Proc(z-lib.org).pdf*. (n.d.).
- Abhinav, K., & Annamalai, K. (2013). *ER ER*. *2*(1), 1–5.
- Ahmed, G. M. S., Ahmed, H., Mohiuddin, M. V., & Sajid, S. M. S. (2014). Experimental Evaluation of Springback in Mild Steel and its Validation Using LS-DYNA. *Procedia Materials Science*, *6*(Icmpc), 1376–1385. https://doi.org/10.1016/j.mspro.2014.07.117
- ASTM E8. (2010). ASTM E8/E8M standard test methods for tension testing of metallic materials 1. *Annual Book of ASTM Standards 4*, *i*(C), 1–27. https://doi.org/10.1520/E0008
- Billade, B. R., & Dahake, P. S. K. (2018). Optimization of Forming Process Parameters in Sheet Metal Forming Of Reinf-Rr End Upr-Lh / Rh for Safe Thinning. *Journal of Engineering Research and Application*, *8*(8), 1–7.
- Biradar, A., & Deshpande, M. D. (2012). Finite Element Analysis of Springback of a Sheet Metal in Wipe Bending Process. *International Journal of Science and Research (IJSR) ISSN (Online Impact Factor*, *3*(7), 2319–7064. Retrieved from www.ijsr.net
- Boljanovic, V. (2004). *Sheet metal forming processes and die design*. 219.
- Buang, M. S., Abdullah, S. A., & Saedon, J. (2015). Effect of die and punch radius on springback of stainless steel sheet metal in the air V-die bending process. *Journal of Mechanical Engineering and Sciences*, *8*(January 2016), 1322–1331.
- Catalog, P. (2015). *Perforated Metal & Expanded Metal*.
- Catalogue, R. P. (n.d.). *Perforation without limits*.
- Chen, F. K. (1993). Analysis of plastic deformation for sheet metals with circular perforations. *Journal of Materials Processing Tech.*, *37*(1–4), 175–188.
- Choudhury, I. A., & Ghomi, V. (2014). Springback reduction of aluminum sheet in V-bending dies. *Proceedings of the Institution of Mechanical Engineers, Part B: Journal of Engineering Manufacture*, *228*(8), 917–926. https://doi.org/10.1177/0954405413514225
- Coër, J., Laurent, H., Oliveira, M. C., Manach, P.-Y., & Menezes, L. F. (n.d.). Detailed experimental and numerical analysis of a cylindrical cup deep drawing. *Submitted to International Journal of Material Forming*, 1–42.
- Cui, X., Zhang, Z., Yu, H., Xiao, X., & Cheng, Y. (2019). Springback calibration of a u-shaped electromagnetic impulse forming process. *Metals*, *9*(5), 1–12.

- Dametew, A. W., & Gebresenbet, T. (2016). Numerical Investigation of Spring Back on Sheet. *Global Journal of Researches in Engineering: A Mechanical and Mechanics Engineering*, *16*(4).
- Davis, J. (2001). Alloying: understanding the basics-Light Metals and Alloys. *Materials Science and Technology*, 192–203. https://doi.org/10.1361/autb2001p351
- Dilip Kumar, K., Appukuttan, K. K., Neelakantha, V. L., & Naik, P. S. (2014). Experimental determination of spring back and thinning effect of aluminum sheet metal during L-bending operation. *Materials and Design*.
- Elangovan, K., & Narayanan, C. (2010). Application of Taguchi approach on investigation of formability for perforated Al 8011 sheets. *International Journal of Engineering, Science and Technology*, *2*(5), 300–309. https://doi.org/10.4314/ijest.v2i5.60170
- Elangovan, K., Sathiya Narayanan, C., & Narayanasamy, R. (2010). Modelling of forming limit diagram of perforated commercial pure aluminium sheets using artificial neural network. *Computational Materials Science*, *47*(4), 1072–1078.
- *European Perforators Association*. (n.d.).
- Farsi, M. A., & Arezoo, B. (2011). Bending force and spring-back in V-die-bending of perforated sheet-metal components. *Journal of the Brazilian Society of Mechanical Sciences and Engineering*, *33*(1), 45–51.
- Gite, R. E., Phad, K. S., & Bajaj, D. S. (2016). *Spring Back Effect Analysis of Bracket Using Finite Element Analysis*. *3*(1), 246–255.
- Gupta, M. S., & Reddy, D. R. (2017). Design and analysis of aircraft sheet metal for spring back effect. *Materials Today: Proceedings*, *4*(8), 8287–8295.
- Hirsch, J. (2014). Recent development in aluminium for automotive applications. *Transactions of Nonferrous Metals Society of China (English Edition)*, *24*(7), 1995–2002. https://doi.org/10.1016/S1003-6326(14)63305-7
- Iii, W. P. R. (2018). Metalworking: Sheet Forming. In *Metalworking: Sheet Forming* (Vol. 14). https://doi.org/10.31399/asm.hb.v14b.9781627081863
- Inava Suchy. (1965). In Reply: Behaviour Therapy. In *Hand Book of Die Design* (Vol. 111). https://doi.org/10.1192/bjp.111.479.1009-a
- Jayakumar, N. (2017). *International Journal of Education and Science Research A Review Paper on Forming Process of Perforated Sheet*. (June 2016), 0–8.

- Jo, M., Hwan, Y., & Ho, Y. (2009). Equivalent Material Properties of Perforated Structure for Free Vibration Analysis. *Modal Analysis*, (SMiRT 20), 1–8.
- Joshi, A. R., Kothari, K. D., & Jhala, R. L. (n.d.). *ER*.
- Kaneriya, N., Shah, D., Rana, R., Shah, V., Thakkar, P., Vadodara, M. U., … Vadodara, M. U. (2017). *International Journal of Advance Engineering and Research Finite Element Analysis of Perforated Sheet Metal (PSM) For Optimum Forming Process*. 506–511.
- Khamis, N. A., & Bahari, A. R. (2016). *Mild Steel Sheet Metal Forming using Abaqus Software : Influence of Drawbeads in Minimize Springback*. *11*(20), 11888–11893.
- Kothari, K. D., & Jhala, R. L. (2016). Investigation and parametric analysis of steel perforated sheet metal (PSM) for optimum forming process. *International Journal of Engineering Research in Africa*, *21*, 118–123.
- Liao, H. C. (2006). Multi-response optimization using weighted principal component. *International Journal of Advanced Manufacturing Technology*, *27*(7–8), 720–725. https://doi.org/10.1007/s00170-004-2248-7
- Ling, J. S., Abdullah, A. B., & Samad, Z. (2016). *Application of Taguchi method for predicting Springback in V-bending of aluminum alloy AA5052 strip*. *3*(7), 91–97.
- Member, E. T. A., Matlou, K., & Member, S. A. A. (2013). *Characterising the Effect of Springback on Mechanically Formed Steel Plates*. *I*, 5–8.
- Miranda, S. S., Barbosa, M. R., Santos, A. D., Pacheco, J. B., & Amaral, R. L. (2018). Forming and springback prediction in press brake air bending combining finite element analysis and neural networks. *Journal of Strain Analysis for Engineering Design*, *53*(8), 584–601. https://doi.org/10.1177/0309324718798222
- Mironovs, V., Tatarinov, A., & Gorbacova, S. (2017). Expanding Application of Perforated Metal Materials in Construction and Architecture. *IOP Conference Series: Materials Science and Engineering*, *251*(1). https://doi.org/10.1088/1757-899X/251/1/012027
- Nandedkar, V. M., Chikalthankar, S. B., & Naikwade, S. G. (2015). Factors Affecting on Residual Stresses & Springback in Sheet Metal Bending : A Review. *International Journal for Scientific Research and Development*|, *3*(08), 258–262.
- Narayanan, S. (2012). Influence Of Hole Size, Hole Shape And Hole Pattern On Spring-Back Effect In Perforated Sheet Metals Using FEM. *International Journal of Engineering Science and Technology*, *4*(6), 2636–2640.

- Pal, B. P., & Rao, D. R. (2016). Analytical and experimental evaluation of spring back effects in a typical cold rolled sheet. *International Journal of Mechanical Engineering and Technology*, *7*(1), 119–130.
- Panda, N., & Pawar, R. S. (2018). Optimization of Process Parameters Affecting on Spring-Back in V-Bending Process for High Strength Low Alloy Steel HSLA 420 Using FEA (HyperForm). *International Journal of Aerospace and Mechanical Engineering*, *12*(1), 28–34.
- Panthi, S. K., Ramakrishnan, N., Ahmed, M., Singh, S. S., & Goel, M. D. (2010). Finite Element Analysis of sheet metal bending process to predict the springback. *Materials and Design*, *31*(2), 657–662. https://doi.org/10.1016/j.matdes.2009.08.022
- Perforated Metal. (n.d.). *New Metals Inc.*, 1–36.
- *Perforated metal made to measure – individual and fast*. (n.d.).
- Prabhakar, A., Haneef, M., & M, S. A. R. (2013). Sheet metal forming analyses with spring-back deformation on U-Bends in Isotropic plates. *INternational Journal of Innovative Research in Science, Engineering and Technology*, *2*(9), 4905–4913.
- Practise, M. F. (n.d.). *Heinz Tschaetsch Metal Forming Practise*.
- Reddy, A. C. S., Rajesham, S., Reddy, P. R., Kumar, T. P., & Goverdhan, J. (2015). *An experimental study on effect of process parameters in deep drawing using Taguchi technique*. *7*(1), 21–32.
- Republic, C. (n.d.). *Perforated Metal Sheets Perforated Metal Sheets Expanded Metal*.
- Sayed, A. M. (2019). Numerical analysis of the perforated steel sheets under uni-axial tensile force. *Metals*, *9*(6), 1–16. https://doi.org/10.3390/met9060632
- Shariff, M., Bin, Z., & Awal, A. (2016). *An Investigation on Crack Alleviation in Bending of Aluminium 2024 for An Investigation on Crack Alleviation in Bending of Aluminium 2024 for Aircraft Application*. (June).
- *Specifiers And Buyers Handbook For Perforated Metals*. (1993).
- Ștefan, M., Gheorghe, N., Dan, C., & Mangeron, D. (n.d.). *the Springback Analyse on Sheet Aluminum V Bending Using an Systemic Analysis on Bending Operation*. 178–184.
- Systems, A., & Academy, M. T. (n.d.). *Mechanical Simulation of Metal Perforated Sheets in Facades*. 1–4.
- Technology, M. P., Manufacturing, N. S., Avenue, N., Systems, I., & Engineering, M.

(1993). *Mathematical modeling of plane-strain bending of sheet and plate*. *39*, 279–304.

- Thipprakmas, S. (2010). Finite Element Analysis on V-Die Bending Process. *Finite Element Analysis*. https://doi.org/10.5772/10220
- Thipprakmas, S., & Phanitwong, W. (2011). Process parameter design of spring-back and spring-go in V-bending process using Taguchi technique. *Materials and Design*, *32*(8–9), 4430–4436. https://doi.org/10.1016/j.matdes.2011.03.069
- Trzepiecinski, T., & Lemu, H. G. (2017a). Effect of computational parameters on springback prediction by numerical simulation. *Metals*, *7*(9), 1–14.
- Trzepiecinski, T., & Lemu, H. G. (2017b). Prediction of springback in V-die air bending process by using finite element method. *MATEC Web of Conferences*, *121*, 1–8. https://doi.org/10.1051/matecconf/201712103023
- Uniyal, S. L., Jain, A., Soni, L. R., & Venkatachalam, G. (2016). *Springback Analysis of Perforated Steel*. (6), 140–147.
- Venkatachalam, G., Narayanan, S., & Sathiya Narayanan, C. (2012). Prediction of limiting strains for square pattern - Square hole perforated commercial pure aluminium sheets. *Advanced Materials Research*, *548*, 382–386.
- Venkatachalam, G., Nishanth, J., Mukesh, M., & Pavan Kumar, D. S. (2016). Study of Forming Behaviour of Square Hole Mild Steel Perforated Sheet Metal. *Applied Mechanics and Materials*, *852*, 218–228. https://doi.org/10.4028/www.scientific.net/amm.852.218
- Zhang, D. J., Cui, Z. S., Chen, Z. Y., & Ruan, X. Y. (2007). An analytical model for predicting sheet springback after V-bending. *Journal of Zhejiang University: Science A*, *8*(2), 237–244. https://doi.org/10.1631/jzus.2007.A0237
- Zhang, M., Tian, X., Li, W., & Shi, X. (2018). An equivalent calculation method for press-braking bending analysis of integral panels. *Metals*, *8*(5).

8. APPENDICES

Appendix A

Important specifications of SPECTROMAXx metal analyzers

Model	: SPECTROMAXx Ametek
Weight	: 70 kg
Transport length	: 0.4 m
Transport width	: 0.7 m
Transport height	: 0.6 m
Memory size	: 10000000 MB
Current source	: N
OES/RFA	: OES
Wavelength max.	: 160-800 Nm

Appendix B

Important specifications universal testing machines (Servo-hydraulic)

Model	: Erie DI-CP
Set of wedges for round specimens	: between 8 and 28 mm
Set of wedges for flat specimens	: between 0 and 25 mm.
Set of compression plates	: Ø160 mm.
Electronic extensometer	: EXM-1002
PC control and measurement cabinet	: (computer, monitor, keyboard, and mouse)
The tensile test areas	: between 800 and 1800 mm
The compression/bending test area	: between 1600 and 2000 mm
Height	: 3300 mm
Spring return piston	: 300 mm stroke
Available load capacity	: 400 kN; 600 kN; 1000 kN and 2000 kN

Appendix C

Result of the tensile test

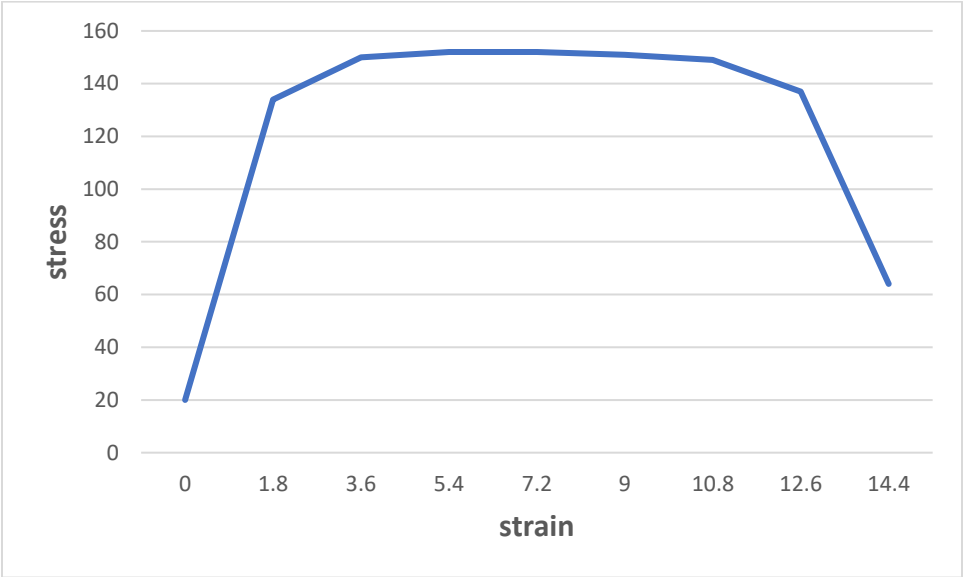

Appendix D

Specifications of Hydraulic Press Brake Machine (WC67Y-160X3200)

Model No.	WC67Y-160/3200
Normal Pressure (k.N)	: 1600 k.N
Working Table Length(mm)	: 3200 mm
Distance Between Housing	: 2600 mm
Throat Depth (mm)	: 320 mm
Side stroke (mm)	: 200 mm
Max. open height (mm)	: 470 mm
Working Speed	: 8 mm
Motor Power	: 11 kW
Packing Size(cm)	: 326x146x264